

**Modeling of pulse–echo inspections of multi–layer panels containing
delaminations**

by

Nathaniel Lawrence Richter

A thesis submitted to the graduate faculty
in partial fulfillment of the requirements for the degree of
MASTER OF SCIENCE

Major: Engineering Mechanics

Program of Study Committee:
R. Bruce Thompson, Major Professor
Timothy Gray
Thomas Rudolphi

Iowa State University

Ames, Iowa

2010

Copyright © Nathaniel Lawrence Richter, 2010. All rights reserved.

DEDICATION

I wish to dedicate this thesis to Erin, my wife, without whose support, understanding, and patience I would not have been able to complete this work. I would also like to thank my friends and family for their guidance and assistance during the writing of this work.

TABLE OF CONTENTS

LIST OF TABLES	vi
LIST OF FIGURES	vii
CHAPTER 1. INTRODUCTION	1
1.1 Background	1
1.2 Problem Statement	2
CHAPTER 2. REVIEW OF LITERATURE	4
2.1 Introduction	4
2.2 Modeling	4
2.3 Material Properties	9
2.4 Conclusion	10
CHAPTER 3. METHODS	12
3.1 Introduction	12
3.2 Transducer Characterization	12
3.2.1 Characterization Setup	12
3.2.2 Characterization Execution and Results	14
3.3 Material Properties Measurements	15
3.3.1 Velocity and Density	15
3.3.2 Attenuation Coefficient	15
3.3.3 Material Properties and Configuration	17
3.4 Thompson–Gray Model Implementation	19
3.4.1 Multiple Layers	19

3.4.2	Reference Frequency Domain Response	19
3.4.3	Transmission and Reflection Ratio	20
3.4.4	Diffraction Correction Ratio	21
3.4.5	Attenuation Ratio	21
3.4.6	Phase Ratio	21
3.5	Implementation Validation	22
3.5.1	Phase Validation	22
3.5.2	Equivalent Path Collision Validation	24
3.5.3	Attenuation and Diffraction Validation	25
3.6	Inspection through Carbon Fiber Surface	27
3.6.1	Inspection Plan Deficiencies	28
3.6.2	Inspection Plan Development	28
CHAPTER 4. RESULTS		33
4.1	2.25 MHz Inspection Model	33
4.1.1	Transducer A	33
4.1.2	Transducer B	34
4.1.3	Transducer C	35
4.2	5 MHz Inspection Model	36
4.2.1	Transducer A	37
4.2.2	Transducer B	38
4.2.3	Transducer C	39
4.3	10 MHz Inspection Model	40
4.3.1	Transducer A	40
4.3.2	Transducer B	41
4.3.3	Transducer C	42
4.4	Flaw Amplitudes	43
CHAPTER 5. DISCUSSION		45
5.1	Experimental Data and the Model	45

5.1.1	Lack of Compaction	45
5.1.2	Adhesive Layer	46
5.1.3	Defect Size	46
5.2	Inspection Plan Motivated by Simulations	46
5.2.1	Comparison of Signal Amplitudes	46
5.2.2	Frequency	46
5.2.3	Focal Length	47
CHAPTER 6. CONCLUSION		48
BIBLIOGRAPHY		50
APPENDIX A. GEOMETRIC FOCAL LENGTH AND EFFECTIVE DI-		
AMETER DATA		52
A.1	Transducer Spectra	52
A.2	Effective Diameter and Geometric Focal Length as a function of diameter. . . .	52
APPENDIX B. ATTENUATION COEFFICIENT MEASUREMENTS . . .		55
APPENDIX C. COLLECTED PROGRAMS AND FUNCTIONS		58
C.1	EQUIVILENT LAYER THICKNESS	58
C.2	ECHO PATH CONSTRUCTOR	59
C.3	REFLECTION AND TRANSMISSION FUNCTION	62
C.4	SPIKE GENERATOR	63
C.5	Diffraction Correction Call Function	65
APPENDIX D. MULTI-LAYER PROGRAM		66
APPENDIX E. TRANSFER MATRIX PROGRAM		76

LIST OF TABLES

Table 3.1	Transducer Physical Characteristics	14
Table 3.2	Measured Transducer Characteristics	15
Table 3.3	Material Properties	17
Table 3.4	Material Properties for Validation	25
Table 3.5	Modeled Transducer Properties	29
Table 4.1	Flaw Amplitudes	43

LIST OF FIGURES

Figure 1.1	Typical Armor Signal	2
Figure 2.1	Pulse–echo inspection with small flaw	5
Figure 2.2	Pulse–echo inspection with large flaw	7
Figure 2.3	Pulse–Echo Reference Measurement Setup	9
Figure 2.4	Pulse–Echo Reference Measurement of Fused Quartz	10
Figure 2.5	Pulse–Echo attenuation measurement configuration	11
Figure 3.1	Alignment of Transducer for Characterization	13
Figure 3.2	Through Transmission Setup	16
Figure 3.3	Armor Layer Configuration	18
Figure 3.4	Echo Path Examples	20
Figure 3.5	Transfer Matrix Generated Reference Signal	23
Figure 3.6	Phase Validation	24
Figure 3.7	Collision Graph	25
Figure 3.8	Attenuation and Diffraction Graphical Validation	26
Figure 3.9	Model and Experimental Data Comparison 1	27
Figure 3.10	Model and Experimental Data Comparison 2	28
Figure 3.11	Undamaged Signal	29
Figure 3.12	Damaged Signal	30
Figure 3.13	Reference Signal: 2.25 MHz	31
Figure 3.14	Reference Signal: 5 MHz	31
Figure 3.15	Reference Signal: 10 MHz	32

Figure 4.1	Unflawed Simulation: 7.5 in. focus at 2.25 MHz	33
Figure 4.2	Flawed Simulation: 7.5 in. focus at 2.25 MHz	34
Figure 4.3	Unflawed Simulation: 8.5 in. focus at 2.25 MHz	34
Figure 4.4	Flawed Simulation: 8.5 in. focus at 2.25 MHz	35
Figure 4.5	Unflawed Simulation: 9.5 in. focus at 2.25 MHz	35
Figure 4.6	Flawed Simulation: 9.5 in. focus at 2.25 MHz	36
Figure 4.7	Unflawed Simulation: 7.5 in. focus at 5 MHz	37
Figure 4.8	Flawed Simulation: 7.5 in. focus at 5 MHz	37
Figure 4.9	Unflawed Simulation: 8.5 in. focus at 5 MHz	38
Figure 4.10	Flawed Simulation: 8.5 in. focus at 5 MHz	38
Figure 4.11	Flawed Simulation: 9.5 in. focus at 5 MHz	39
Figure 4.12	Flawed Simulation: 9.5 in. focus at 5 MHz	39
Figure 4.13	Unflawed Simulation: 7.5 in. focus at 10 MHz	40
Figure 4.14	Flawed Simulation: 7.5 in. focus at 10 MHz	41
Figure 4.15	Unflawed Simulation: 8.5 in. focus at 10 MHz	41
Figure 4.16	Flawed Simulation: 8.5 in. focus at 10 MHz	42
Figure 4.17	Unflawed Simulation: 9.5 in. focus at 10 MHz	42
Figure 4.18	Flawed Simulation: 9.5 in. focus at 10 MHz	43
Figure 4.19	Flaw Amplitude	44
Figure 4.20	Flawed to Unflawed Ratio	44
Figure A.1	Probe Spectra	52
Figure A.2	Transducer 663762	53
Figure A.3	Transducer 663763	53
Figure A.4	Transducer 664645	54
Figure A.5	Transducer 664646	54

ACKNOWLEDGEMENTS

I would like to take this opportunity to express my thanks to those who helped me with various aspects of conducting research and the writing of this thesis. First and foremost, Dr. R. Bruce Thompson and Dr. Frank Margetan for their guidance, patience, and assistance throughout this research and the writing of this thesis. I would also like to thank my committee, Dr. Timothy Gray and Dr. Thomas Rudolphi, for their assistance with my research and throughout my graduate education.

ABSTRACT

To meet the needs of counter insurgency operations the armor of tanks need to be lighter. This is accomplished by using a combination of materials: metals, composites, and ceramics. This multi-material composite armor using any combination of the above materials will need to be inspected for manufacturing error, shipping damage, and combat damage. Nondestructive inspection, particularly ultrasonic inspection, has a long history of successfully inspecting thick composite structures.

To more easily develop inspection plans for many layered composites a computational model would be of use. A model of this type would need to have the ability to account for multiple material types and flaws that are larger than the beam size. Also, as a result of armor thickness any model would need to consider attenuation and effects of focused transducers.

This was accomplishing by extending the Thompson–Gray Measurement Model for use with multiple layers at normal incidence to the transducer and large planar defects parallel to the layers. Material values of the armor and the characteristics of the transducers were determined for use in the model. The model results are compared to experimentally collected data to show agreement. The model is then used to determine the requirements of a new inspection plan through varying the frequency and focal length of the transducers.

The defect reflection amplitudes for 5 MHz with the focal lengths in water of 7.5, 8.5, and 9.5 inches are 0.55178, 0.75270, and 0.44836. The same for 10 MHz are 0.12474, 0.21425, and 0.10637.

The 8.5 in focal length also is the equivalent thickness in water for the material leading to the defect interface. This focal length would, from theory, cause the greatest amplitude from the defect. This is supported by the results in that the highest amplitude occurs at 8.5 inches

for both sets of frequencies. It is also evident that the response at 5 MHz is greater than that at 10 MHz. As such, the 5 MHz transducer with an 8.5 inch focal length is nominal for this inspection.

CHAPTER 1. INTRODUCTION

1.1 Background

In the World War II and Cold War eras armored vehicles dominated the battlefield due to their combination of toughness, firepower, and mobility. With the end of the Cold War and the advent of the "War on Terror", conventional armor has lost its pride of place among weapon systems because of their high operational costs and the tactical shift toward greater mobility. [Cheeseman et al. \(2004\)](#)

To achieve improved cost performance and greater mobility, a net reduction in weapon system weight needs to occur with the mostly likely reductions occurring with the armor. This returns to the reoccurring decision of sacrificing protection for greater speed and range. There is now, however, a solution: composite armor. More specifically, armor made out of a combination of traditional composites, ceramics, and metals. In this way, system speed and range can be increased while providing comparable or greater protection to the system operators.

Armor of this type will, like traditional composites, have portions that are completely obscured from visual inspection. This leads to the requirements of how to implement quality control for the manufacturer, how to determine delivery acceptability for the end user, and how to determine fitness of use after potential damage. Established methods of nondestructive evaluation, namely ultrasonic inspection, have a long history of meeting requirements such as those listed above for many engineered systems.

1.2 Problem Statement

Ultrasonic inspection has been used for many years to inspect metals, composites, and ceramics individually with much success due to the relatively straight forward nature of inspection techniques and the signal of the response.

When considering a specimen composed of multiple material types layered together in varying thicknesses; it is often the case in practice that a complex ultrasonic response will result, as seen in [Figure 1.1](#).

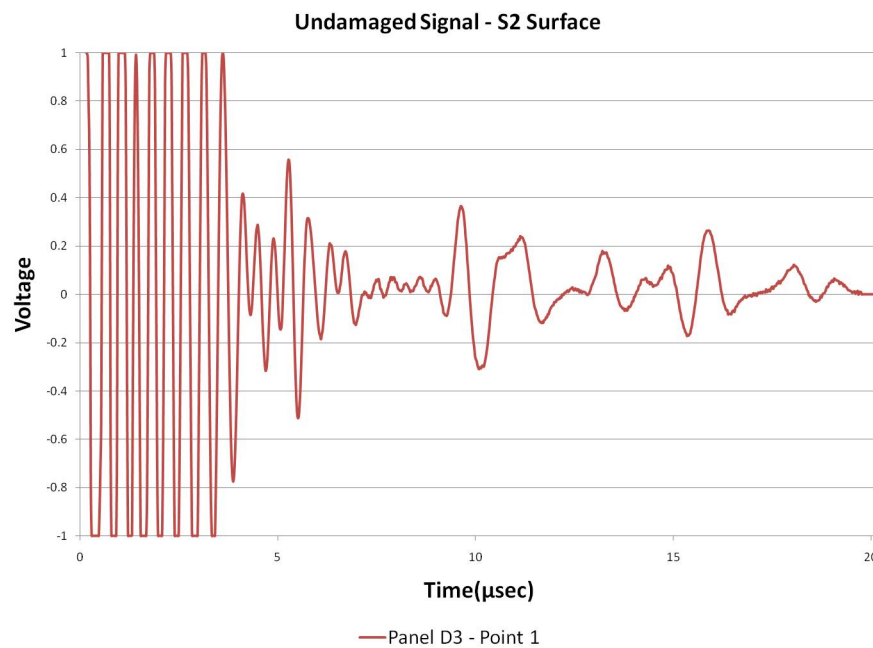


Figure 1.1 Pulse/echo ultrasonic response observed in an unflawed 5-layer composite armor panel. A 2.25 MHz, 1.5 in. diameter, 5 in. focal length was used (olympus 664646) with a waveform sampled at a 100 MHz rate.

This complexity will easily impede the ability of the manufacturers and customers to accurately inspect not only the interior of the layers but the bond line between layers as well. This is caused by the complex signal through increasing the difficulty of determining defect location. With the aid of ultrasonic modeling, it will be possible to identify defect signals among the layer responses.

The specific aim of this work is to develop a model capable of predicting time domain signals as seen in [Figure 1.1](#) for both the unflawed and flawed cases where the flaws are disbonds larger than the beam diameter. Due to the the thickness of the panels and the materials used, attenuation must be considered. In order to improve the signal to noise ratio a focused transducer is needed to conduct the inspections. As a result, the model will be required to account for both attenuation and the effects of a focusing transducer.

After the model is validated, it will be used to simulate different inspections by varying the transducer frequency and focal length. In this way nominal transducer characteristics can be determined for the inspection of a defect along a specified bond plane.

CHAPTER 2. REVIEW OF LITERATURE

2.1 Introduction

This section will be devoted to the review of literature that describes modeling methods and theory that will meet the criterion set out in the problem statement.

2.2 Modeling

In the field of ultrasonics, there exist many possible models for ultrasonic response. One of the first models for the transmission through and reflection from parallel layers was derived by Thomson (1950). Beginning from the general equations of displacement and stress in terms of both dilatation and rotation Thomson derives the recurrence formula for the general longitudinal and shear wave case. In this way, a single transfer matrix models each layer and its interactions and the product of the individual matrices in turn models the multi-layered assembly.

$$[t_i] = \begin{bmatrix} \cos(k_i z_i) & j Z_i \sin(k_i z_i) \\ \frac{j}{Z_i} \sin(k_i z_i) & \cos(k_i z_i) \end{bmatrix}$$

Here i denotes the layer, Z_i is the acoustic impedance of the layer, k_i is the wave number for the layer, and z_i is the layer thickness.

$$[T] = [t_1] \cdot [t_2] \cdot [t_3] \cdot \dots$$

From the matrix, $[T]$, the reflection and transmission coefficients can be determined for the assembly as follows:

$$[T_{armor}] = \begin{bmatrix} A & B \\ C & D \end{bmatrix}$$

$$S_{11} = \frac{A + B/Z - C \cdot Z - D}{A + B/Z + C \cdot Z + D}$$

$$S_{21} = \frac{2}{A + B/Z - C \cdot Z - D}$$

In this way, the reflection, S_{11} , and transmission, S_{12} , coefficients can be computed as a function of frequency.

A more recent method of ultrasonic modeling was put forth by [Thompson and Gray \(1983b\)](#). This method considers an immersion inspection of a single layer containing a flaw. Auld's reciprocity formula and the quasi-planar assumption are used to derive a relationship for the ultrasonic scattering from a small reflector in a solid medium, [Figure 2.1](#), for a piston transducer in pitch-catch configuration which can be reduced to the pulse-echo case by taking the receiver to be the transmitter.

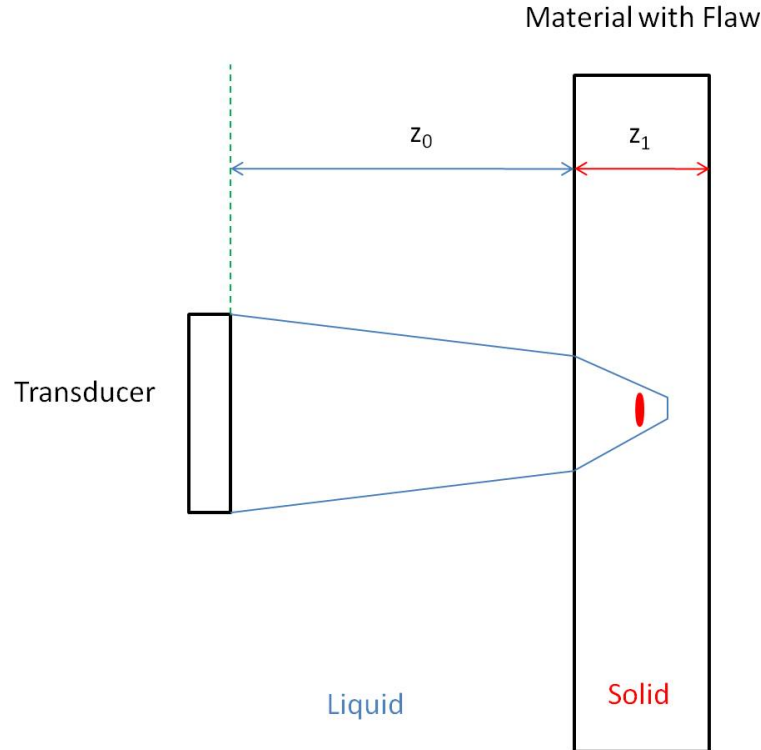


Figure 2.1 The figure is the setup of a simple pulse-echo measurement with the transducer normal to the material surface. The flaw in the solid layer is smaller than the beam size.

The primary result from the signal from the flaw is that:

$$\begin{aligned} \delta\Gamma_F &= \beta T_a T_b C_a C_b \frac{2A^* \rho_1 v_b}{ik_b a^2 \rho_0 v_0} \\ &\times \exp[-i(k_0(z_{0a} + z_{0b}) + k_a z_{1a} + k_b z_{1b})] \\ &\times \exp[-(\alpha_0(z_{0a} + z_{0b}) + \alpha_a z_{1a} + \alpha_b z_{1b})] \end{aligned} \quad (2.1)$$

This equation can be written in the following form for pulse-echo measurements:

$$\delta\Gamma_F = \beta [T_{01} R_{11} T_{10}]_F C^2 \quad (2.2)$$

$$\begin{aligned} &\times \underbrace{\frac{2A^* \rho_1 v_1}{ik_1 a^2 \rho_0 v_0}}_{\text{Flaw Scatter}} \\ &\times \underbrace{\exp[-i2(k_0 z_0 + k_1 z_1)]}_{\text{Phase}} \\ &\times \underbrace{\exp[-2(\alpha_0 z_0 + \alpha_1 z_1)]}_{\text{Attenuation}} \end{aligned} \quad (2.3)$$

Here $\delta\Gamma_F$ is the change in response due to the presence of a flaw, $[T_{01} R_{11} T_{10}]_F$ are the reflection and transmission coefficients at the liquid-solid interface, β is related to the transducer efficiency, C is the axial pressure variations due to the presence of a flaw that model diffraction, and A^* is the scattering amplitude of the flaw. The material properties of the denoted layers are ρ , the density, v the material velocity, k the wave number, z the layer thickness, and α the attenuation. Subscripts 0 and 1 refer to the water and solid, respectively. This model is appropriate to cases when the flaw is small with respect to the ultrasonic beam as seen in [Figure 2.1](#).

In the case of a large planar defect, [Figure 2.2](#), that can be treated as a perfect reflector, such as a delamination, use of the scattering amplitude is no longer an appropriate approximation. Instead, the flaw signal is modeled totally by the diffraction correction term and the reflection coefficient as seen in [Minachi et al. \(1993\)](#). The assumption of large planar flaws require that the axial pressure variations across the area of the beam are considered to model diffraction, D , rather than only the axial pressure variations, C .

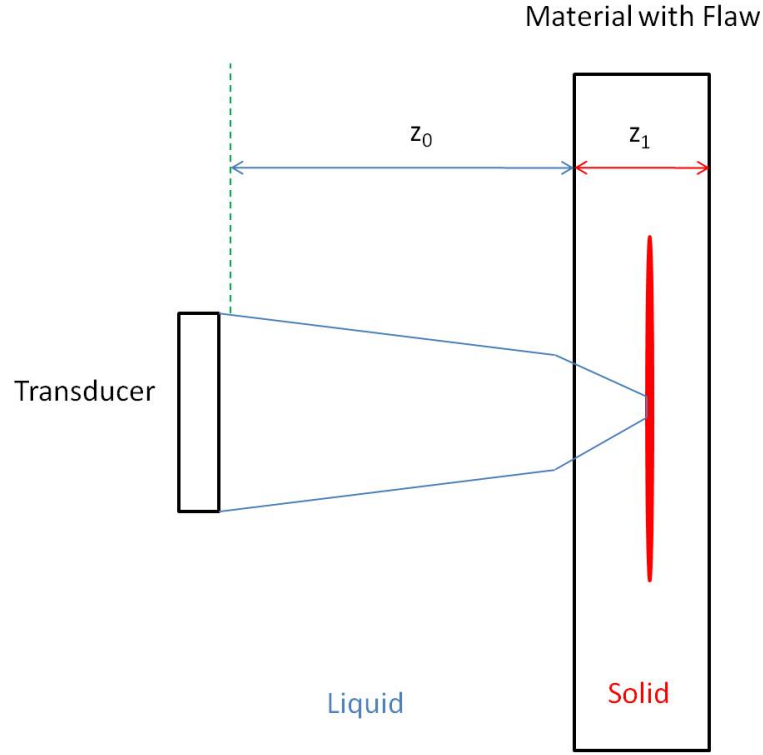


Figure 2.2 The flaw in the solid layer is now much larger than the beam size.

A closer look is required of the diffraction correction term D . As mentioned in [Thompson and Gray \(1983a\)](#) and further illustrated in [Thompson and Gray \(1981\)](#) the diffraction correction terms, D , can be extended from the one medium case to the two medium case such that z_{eqv} is the equivalent material thickness of layer z_1 as though it was composed of the material of layer z_0 .

$$z_{eqv} = z_0 + \frac{v_1}{v_0} z_1 \quad (2.4)$$

$$D(z_0, z_1) = D(2z_{eqv})$$

$$D(s) = 1 - \exp\left(\frac{-2i\pi}{s}\right) \left[J_0\left(\frac{2\pi}{s}\right) + iJ_1\left(\frac{2\pi}{s}\right) \right] \quad (2.5)$$

$$s = \frac{4\pi z_{eqv}}{ka^2} \quad (2.6)$$

Equation 2.5 is the special case for a circular planar transducer. To describe the focusing effects of a transducer the integral of the pressure variations along the interface need to be considered. The integral will be of the following form:

$$D = \int_{Beam\ Area} C^2 dA \quad (2.7)$$

The equivalent path assumption still holds for this more complicated evaluation. The implementation of results in Equation 2.8.

$$\begin{aligned} \delta\Gamma_F = \beta[T_{01}R_{11}T_{10}]_F D \times & \underbrace{\exp[-i2(k_0z_0 + k_1z_1)]}_{Phase} \\ & \times \underbrace{\exp[-i2(\alpha_0z_0 + \alpha_1z_1)]}_{Attenuation} \end{aligned} \quad (2.8)$$

In order to determine the transducer efficiency term, β , a reference measurement needs be made. The measurement takes place in a similar fashion as seen in Figure 2.3. For the reference measurement of this model, a common choice is to select a material that has negligible attenuation, such as fused quartz, that would allow the attenuation term for that layer to vanish.

Figure 2.4 was collected with Transducer 664646, UTEX UT 340 Pulser and Receiver, a six DOF Sonix tank, at 100 MHz sampling rate, 9 dB of gain, and using UTEX Winspect. All experimental data was collected with this equipment but differing gain and sampling rate.

$$\Gamma_R = \beta[T_{01}R_{11}T_{10}]_R D \exp[-i2(k_0z_0 + k_1z_1)] \exp[-i2(\alpha_0Rz_0 + \alpha_1Rz_1)] \quad (2.9)$$

Where Γ_R is the measured amplitude in terms of frequency and D is the diffraction correction term for the planar interface. If the ratio of Equation 2.8 and Equation 2.9 is determined then the term, β cancels.

$$\Gamma_F = \Gamma_R \frac{[T_{01}R_{11}T_{10}]_F D_F \exp[-i2(k_0z_0 + k_1z_1)] \exp[-i2(\alpha_0z_0 + \alpha_1z_1)]}{[T_{01}R_{11}T_{10}]_R D_R \exp[-i2(k_0z_0 + k_1z_1)] \exp[-i2(\alpha_0Rz_0 + \alpha_1Rz_1)]} \quad (2.10)$$

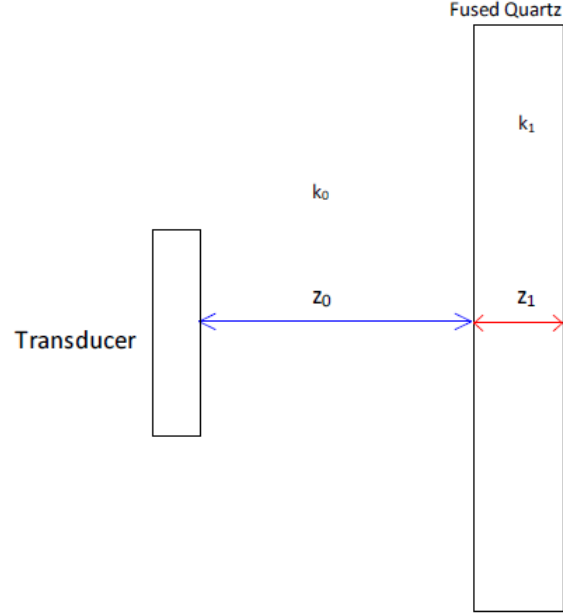


Figure 2.3 Pulse-Echo Reference Measurement Setup: The desired portion of the signal generated is the second echo that corresponds to passing through the layers of water and fused quartz twice.

From the relationship of the equivalent material path seen in [Equation 2.4](#) it should be possible to extrapolate this from two layers to many layers.

2.3 Material Properties

To assemble an accurate computational model there needs to be accurate measurements of material properties. The measurement of velocity through ultrasonic means [ASTME494-05 \(2005\)](#) and the measurement of density for solids are standardized or well known. The most traditional method for measuring attenuation as mentioned in [Panetta et al. \(1995\)](#) is a variation of the pulse-echo method and follows the same form as the model described in [Thompson and Gray \(1983b\)](#).

If [Equation 2.9](#) is applied to the two configurations as shown in [Figure 2.5](#) then the ratio of the two will result in the following equation.

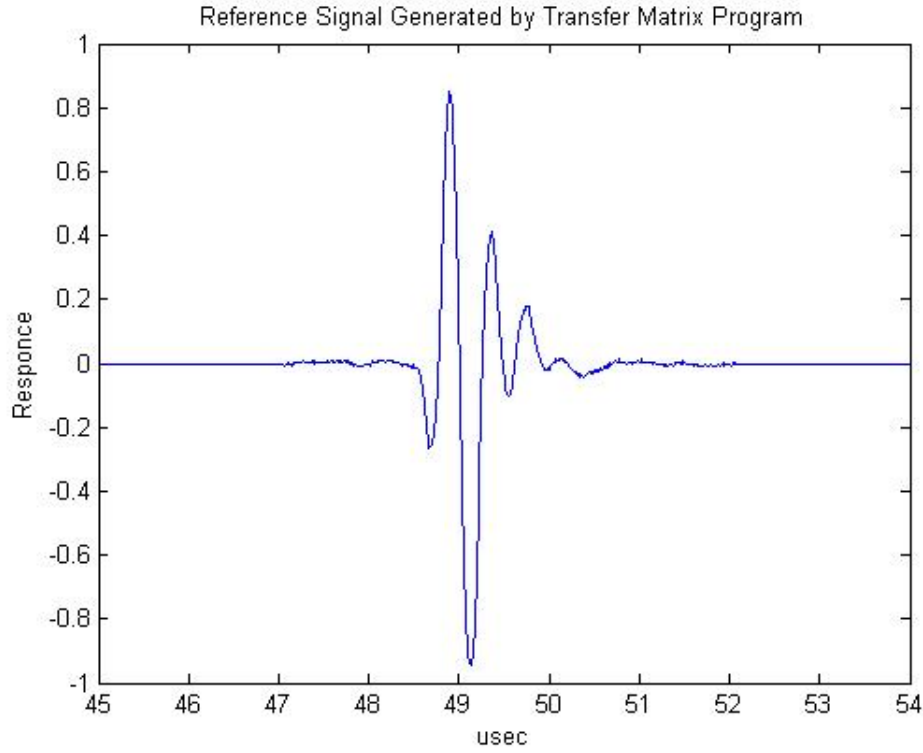


Figure 2.4 Pulse-Echo Reference Measurement of Fused Quartz

$$\frac{\Gamma}{\Gamma_{ref}} = \frac{|T_{01}R_{11}T_{10}|e^{-2\alpha_{unk}z_1-2\alpha_{H_2O}z_0}}{|(T_{01}R_{11}T_{10})_{ref}|e^{-2\alpha_{ref}z_{1ref}-2\alpha_{H_2O}z_{0ref}}} \quad (2.11)$$

The diffraction correction, D as present in Equation 2.9 has canceled for a planar or focused transducer if an equivalent total traveling path is used. The transducer efficiency term, β , has also canceled as previously seen in Equation 2.10. The attenuation caused by water, α_{H_2O} , is has been tabulated extensively according to temperature. These tabular values are used. The unknown attenuation can be solved for, as a function of frequency, through the ratio Equation 2.11.

2.4 Conclusion

When considering the ultrasonic models in light of the problem statement, it becomes evident that the transfer matrix method of Thomson (1950) is insufficient because of its in-

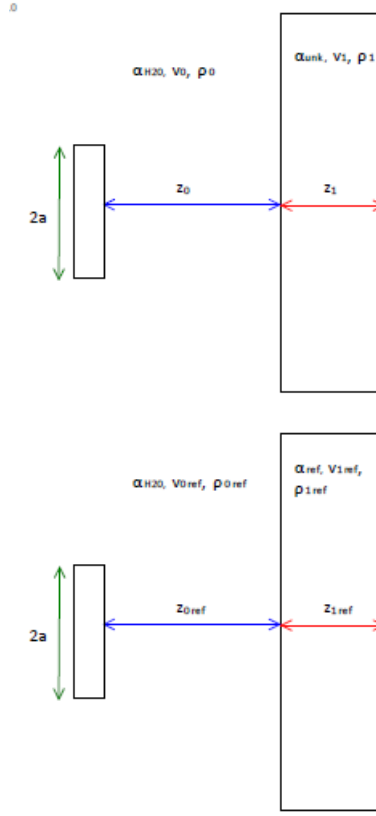


Figure 2.5 Pulse-Echo attenuation measurement configuration: The top portion refers to a measurement on the unknown sample and the bottom part refers to measurements and reference sample for which attenuation, velocity, and density are known.

ability to model diffraction, which is important for modeling focused transducers. While the Thompson–Gray measurement model is fully capable of modeling the effects of material attenuation and diffraction it has not been explained how the model would represent multiple layers of an entire signal. This is explained, in detail in [section 3.4](#).

CHAPTER 3. METHODS

3.1 Introduction

In this chapter, the methods used to implement and test an ultrasonic model are detailed. Many components are required to model a signal as seen in [Figure 1.1](#). The following will be the detailed method used by the author for the determination of those model components. The specific components of interest are divided into two separate groups: material or transducer properties. The values of the variables used for the materials and equipment will be presented. Lastly, the implementation of the model described by [Equation 2.10](#) will be detailed and validation will be presented.

3.2 Transducer Characterization

The method for the characterization of focused transducers that was used is outlined in detail in [Margetan and Thompson \(1994\)](#). This method allows for the determination of the geometric focal length and the effective diameter of the probe. The reason for using these values in favor of the nominal values provided by the manufacturer is that the nominal values do not accurately describe how each transducer focuses. An overview of the steps used by the author to determine these values will be presented and any differences with [Margetan and Thompson \(1994\)](#) will be highlighted.

3.2.1 Characterization Setup

Alignment of the transducer center on the point target is essential for the accurate measurement of the transducer focal length and effective diameter. The following steps assume the use of a stage that is level with respect to two orthogonal axes. The author found it was useful

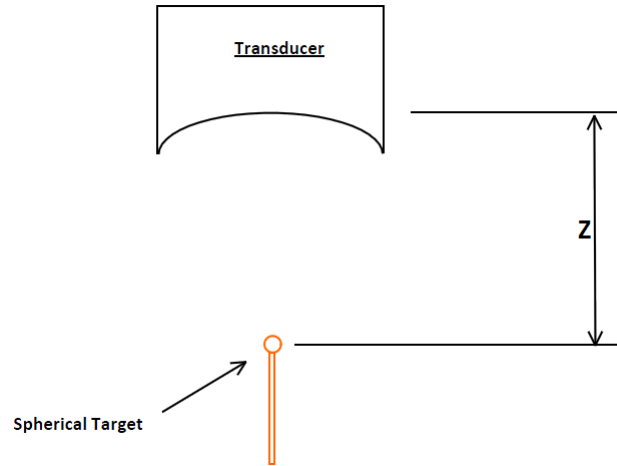


Figure 3.1 Alignment of Transducer for Characterization: The distance, z , is measured from the top of the spherical target to the center of the transducer face. The spherical target used is created by partially melting a glass rod and allowing gravity to pool the glass at one end.

to normalize the transducer, through the rotation of the gimbals, to a flat specimen block. This extra step results in closer initial alignment to the point target. Here a point target can be any small spherical surface such as a ball bearing or a partially melted glass rod with pooled glass at one end. The author made use of the later.

Care was taken to align the central beam axis with the point target in water. This was accomplished by alternately rotating the gimbals and translating along the axes of the plane perpendicular to the z -axis, as defined in [Figure 3.1](#), until any deviation results in an amplitude drop. This alignment was then checked along the z -axis at several points to ensure that any deviation will result in an amplitude decrease. This ensures that the center of the transducer is aligned with the point target.

The next is the collection of response waveforms along the z -axis in ascending order, as seen in [Figure 3.1](#). Here the distance of the transducer face to the target is defined as zero when the transducer face is touching the point target. This is a difference from [Margetan and Thompson \(1994\)](#) where the zero is defined as the distance from the target to the plane created by the edges of the transducer face. This author's definition allows the product of the time

of flight to the geometric focal plane and the material velocity to be equivalent to the focal length. This allows for more convenient experimental setup.

3.2.2 Characterization Execution and Results

The evaluation of the data by programs written by Dr. Margetan based on the theory outlined in [Margetan and Thompson \(1994\)](#). The programs perform a χ^2 , chi-squared, fit of the axially varying pressure, [Equation 3.1](#), between the measured data and the theory by varying the proportionality constant, effective diameter, and the geometric focal length.

$$\Gamma = c' \left(\frac{F}{z_i - F} \sin \left(\frac{\pi(z_i - F)D^2 f}{8vz_i F} \right) e^{-\alpha z_i} \right)^2 \quad (3.1)$$

Here the variables varied for the χ^2 fit are defined as follows: D is the effective diameter, F is the geometric focal length, and c' is the proportionality constant. The other variable not varied for the χ^2 fit are as follows: z_i is the distance from the point target, v is the acoustic water velocity, f is the frequency, α is the attenuation in water.

Transducer	Frequency	Physical Diameter	Nominal Focal Length
663762	2.25 MHz	1.5 in.	2.7 in.
663763	2.25 MHz	1.5 in.	2.7 in.
664645	2.25 MHz	1.5 in.	5.0 in.
664646	2.25 MHz	1.5 in.	5.0 in.

Table 3.1 Transducer Physical Characteristics

Four separate focused transducers have been used in this project. The nominal transducer physical characteristics are located in [Table 3.1](#). The transducers 663762 and 663763 were used mostly for material characterization where the remaining two were used for validation measurements of the armor panels.

The geometric focal length and the effective diameter for all four probes are calculated from the spectra as show in [Appendix A](#). For ease of reference, the average geometric focal length and the effective diameter resulting from the independent fit of the variable are listed in [Table 3.2](#).

Transducer	Effective Diameter	Geometric Focal Length
663762	1.528 in.	2.665 in.
663763	1.557 in.	2.738 in.
664645	1.537 in.	5.356 in.
664646	1.532 in.	5.233 in.

Table 3.2 Transducer Modeling Characteristics

3.3 Material Properties Measurements

In this section, the methods for determining the velocity, density, and attenuation coefficient by the author are outlined. The material properties will be tabulated at the end of the section.

3.3.1 Velocity and Density

The method used to measure the acoustic velocity of materials was the pulse-echo method as outlined by [ASTME494-05 \(2005\)](#). In this simple method, the thickness of the material is measured with a micrometer. The time of flight is determined at normal incidence for an ultrasonic signal in the material. If the measurement is taken where the specimen is submerged then an extra step of subtracting the time of flight due to the water is taken. Lastly, the ratio of the thickness to half the time of flight is the pressure wave velocity of the material.

The density of the material is determined by measuring the mass of a known volume of the material. The resulting ratio of mass to volume results in the density.

3.3.2 Attenuation Coefficient

The setup for the attenuation measurement consist of normalizing the transducers to the surface of the material, the collection of several points of data at differing locations, and the collection of a water reference. Care should be taken to equate or record the gain of the material data and the reference data.

The theory behind the determination of the attenuation coefficient by means of a pulse-echo measurement is described by [Equation 2.11](#). This method can be modified to accommodate through transmission measurements as seen in [Figure 3.2](#).

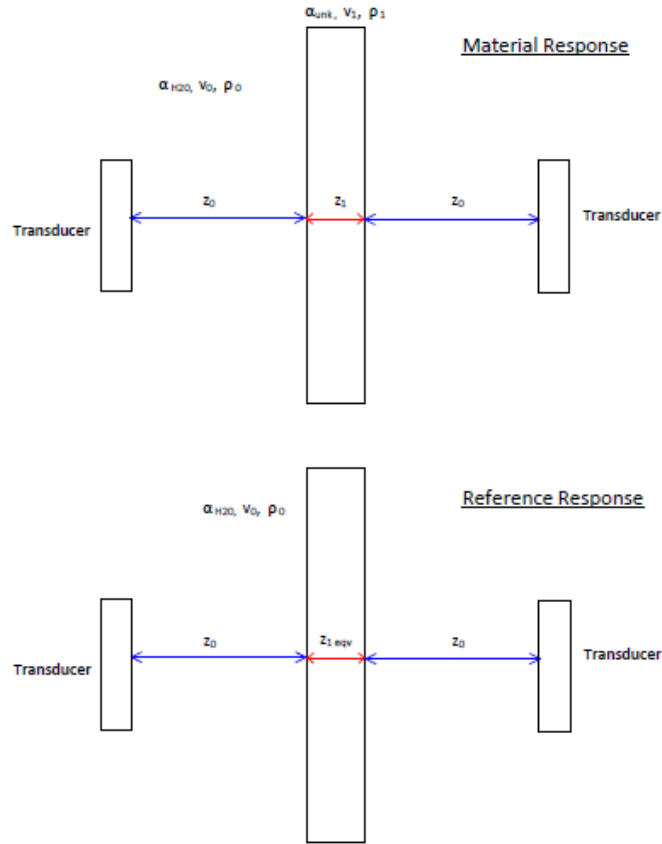


Figure 3.2 The setup for through transmission attenuation measurement where water is the reference. Note that the water paths are the same for both the material with the unknown attenuation and the water only reference.

There are modifications of [Equation 2.11](#) that result in [Equation 3.2](#). The changes in the numerator are the removal of the reflection coefficient and the reduction in the number of times the signal passes through the material that is being measured. Both are a result of the change from pulse-echo to through transmission. The modifications in the denominator are the removal of all transmission and reflection coefficients as well as the replacement of the attenuation term for the reference material with an attenuation term for the materials equivalent thickness of water. If the material sample were very thin then it would be viable to set the equivalent thickness to zero. It can be assumed that the water layer on either side of the material is equal in thickness. If these layers are equal to those in the reference the

attenuation terms for the water path in the numerator and denominator, cancel.

$$\frac{\Gamma}{\Gamma_{ref}} = \frac{|T_{01}T_{10}| e^{-\alpha_{unk}z_1}}{e^{-\alpha_{H_2O}z_{1eqv}}} \quad (3.2)$$

Upon solving Equation 3.2 for α_{unk} we arrive at Equation 3.3.

$$\alpha_{unk} = -\frac{1}{z_1} \left(\ln \frac{\Gamma}{\Gamma_{ref}} \frac{1}{|T_{01}T_{10}|} - \alpha_{H_2O}z_{1eqv} \right) \quad (3.3)$$

Equation 3.3 is the basis used by a MATLAB program to determine the attenuation coefficients as a function of frequency. The program is located in Appendix B. The results of this method, are only valid for frequencies near that of the transducer, and can be fitted to a power law function for later use,

$$\alpha = Cf^p \quad (3.4)$$

where f is the frequency and C and p are values determined by a simple least squares fit.

3.3.3 Material Properties and Configuration

The Table 3.3 lists the material properties of the different layers.

Material	Thickness(cm)	Velocity(cm/ μ s)	Density(g/cm ³)	C	p
S2 Fiberglass	—	0.336	1.78	0.6274	1.2117
Carbon Fiber	—	0.302	2.738	0.1353	1.2198
SiC Ceramic Tile	—	1.224	5.356	0.000	1
Rubber	—	0.155	5.233	1.445	1.0506

Table 3.3 Material properties for the individual layers as determined by the methods outlined in section 3.3. Layers are in no specific order. C is the attenuation coefficient in *Nepers/cm* and p is the power as seen in Equation 3.4.

The layers of the armor panel are arranged in the manner of Figure 3.3. It is obvious that several of the materials in Table 3.3 are anisotropic. Anisotropy, however, is not modeled

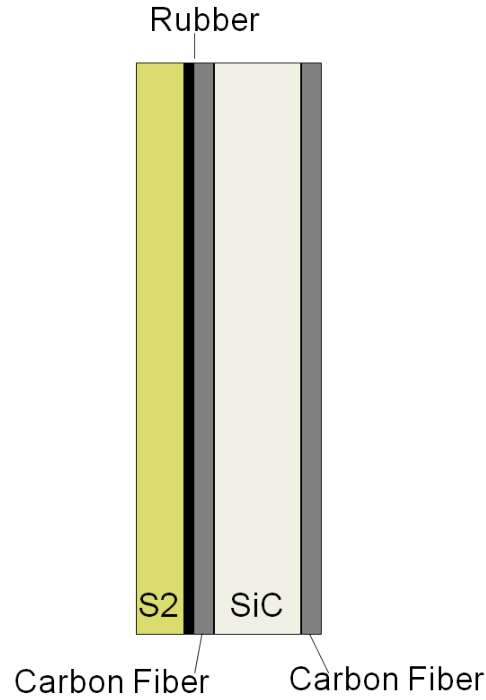


Figure 3.3 The above is the physical ordering of the armor layers.

directly. Instead, the material properties are measured with the same orientation that is present in the full armor panels. In this way, some irregularity due to material anisotropy is modeled.

For modeling a pulse echo inspection from the fiberglass side a layer of water is assumed to exist that is 9.7cm thick, with a density of unity, a velocity of $0.1479\text{cm}/\mu\text{s}$, C is 2.61×10^{-4} , and p is 2. A thin layer of adhesive, FM4, exists between each layer. This adhesive was not modeled directly due to lack of a material specimen for property determination. There also exist technical challenges in modeling many very thin layers. In order to model the time shift caused by the adhesive there was a slight increase (0.04cm) to the values of all composite layers. The production armor panels were also wrapped in a thin layer of S2 fiberglass. This is modeled through its addition to the fiberglass thickness and the inclusion of a separate layer for inspections occurring through the carbon fiber side.

3.4 Thompson–Gray Model Implementation

The implementation of the Thompson–Gray model will be referred to as the Multi-layer Program (MLP). The first step in implementation resides with Equation 2.10 after the implementation of the equivalent path relationship as shown by Equation 2.4.

$$\Gamma_F = \Gamma_R \times \overbrace{\frac{[T_{01}R_{11}T_{10}]_F}{[T_{01}R_{11}T_{10}]_R}}^{\text{Transmission and Reflection Ratio}} \times \overbrace{\frac{D(z_{eqv})_F}{D(z_{eqv})_R}}^{\text{Diffraction Ratio}} \quad (3.5)$$

$$\times \underbrace{\frac{\exp[-2(\alpha_0 z_0 + \alpha_1 z_1)]}{\exp[-2(\alpha_{0R} z_{0R} + \alpha_{1R} z_{1R})]}}_{\text{Attenuation Ratio}} \times \underbrace{\frac{\exp[-i2(k_0 z_0 + k_1 z_1)]}{\exp[-i2(k_{0R} z_{0R} + k_{1R} z_{1R})]}}_{\text{Phase Ratio}}$$

The following subsections will describe how the model is implemented for multiple layers and the components of Equation 3.5.

3.4.1 Multiple Layers

A single evaluation of Equation 3.5 will not result in the modeling of a signal such as Figure 1.1. Rather, such an evaluation will result in the simulated response of a single interface with a specific time of flight. The simulated interface is determined by a sequence of reflection and transmission coefficients leading to and reflecting from the simulated interface. This sequence of coefficients is called an echo path. This concept is also illustrated in Figure 3.4. It can be seen that differing echo paths traverse layers a different number of times. Different echo paths will lead to different times of flight for the response from a given interface. From this all interface responses of a set of layers is developed by evaluating all possible echo paths bound by a maximum time of flight as generated by section C.2. The set of responses is used to develop the model for the corresponding set of layers by summing all amplitude values for a given point in time.

3.4.2 Reference Frequency Domain Response

As mentioned previously the variable Γ_R is the frequency domain response of the reference measurement. This is obtained simply by applying the fast Fourier transform (FFT) to the

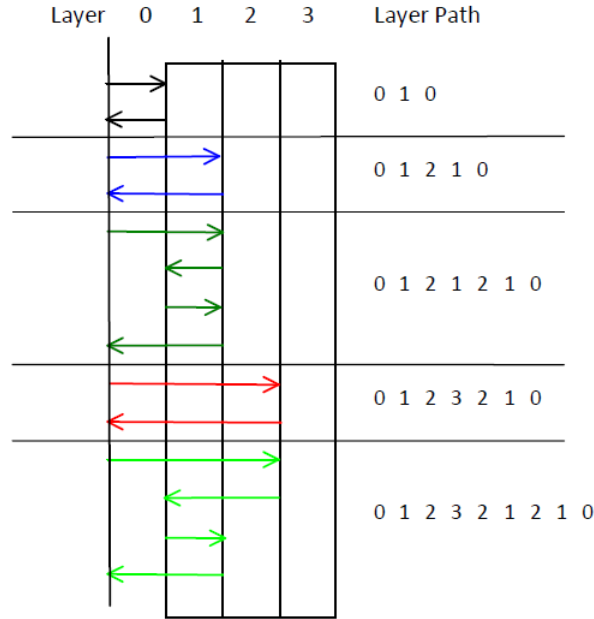


Figure 3.4 Echo Path Examples: Each interface generates either a reflection or a transmission coefficient corresponding to the direction the signal is traveling at that interface.

time domain response of the reference. This is implemented in MATLAB using the FFTW subroutine library as outlined in [Frigo and Johnson \(2005\)](#). The subroutine utilizes the FFT algorithm as described by [Cooley and Tukey \(1965\)](#) when evaluating a data set of N points, here N is a power of two .

The following sections describe the evaluation of each of the factors in [Equation 3.5](#).

3.4.3 Transmission and Reflection Ratio

There are two components of the transmission and reflection ratio. The denominator contains the echo path that corresponds to the reference signal which in this case is the first back wall reflection from the reference block. The numerator is composed of the product of the reflection and transmissions that compose a single echo path of the armor panel. The product of reflection and transmission coefficients is determined from the echo paths using a program written by the author located in [section C.3](#).

3.4.4 Diffraction Correction Ratio

The diffraction ratio is composed of the reference diffraction correction in the denominator and the simulated value in the numerator. Both values are calculated by using a function written by Dr. Margetan that applies the theory as outlined in [Minachi et al. \(1998\)](#) and adapted to MATLAB by the author. The function called by the main program is located in [section C.5](#).

These functions require the equivalent material thickness for all echo paths. This value is calculated for all echo paths by a function as found in [section C.1](#). In this implementation, the number of times the path traverses a layer is recorded and from there the equivalent thickness in terms of water is calculated.

It was noted that it is possible to have two unique echo paths that result in the same equivalent paths. These collisions are created by the signal going through each layer the same number of times for each echo path but in different orders. When considering these collisions it should be confirmed if both paths are needed to model a response accurately.

3.4.5 Attenuation Ratio

The attenuation is a straight forward application of the theory where the attenuation calculation is determined for each layer at all potential frequencies as seen in [Appendix D](#).

3.4.6 Phase Ratio

The phase ratio, unlike the other components of this equation, is not implemented as a direct application of the equation. The main reason is due to convenience of implementation. To create a full signal, the response of each echo path needs to be calculated. If the phase terms are included then the number of points for each response equals the number of points for a specific time of flight. In example, if an arbitrary multi-layer signal extends from zero to 70 μsec then to model an experiment sampled at 100 MHz, the evaluation of each echo path will have 7000 points. This large number of points will greatly increase the run time of any computational model. In contrast, if the phase term is omitted each echo path can be

evaluated using only the number of points needed to describe an echo path response. This is a valid approach because the magnitude of the phase term is zero and only controls the temporal placement of the response.

With the omission of the phase term, a method needs to be developed for aligning the responses in the proper temporal sequence. To accomplish this, the first time point for all equivalent paths needs to be determined. The difference in time between the first point of the reference signal and the time of flight of the reference configuration will result in the span of time the center of the reference signal is shifted from the first point. This difference of the reference signal and the time of flight will be the same for all paths as well. The time of flight of the paths is calculated by the MATLAB function in [3.4.4](#).

$$T_{0path} - TOF_{path} = T_{0ref} - TOF_{ref} \quad (3.6)$$

$$T_{0path} = T_{0ref} - TOF_{ref} + TOF_{path}$$

Where T_{0path} is the first point in time for a given path, T_{0ref} is the first point in time of the reference used, TOF_{path} is the time of flight of each path, and TOF_{ref} is the time of flight of the reference.

With the knowledge of T_{0path} it is now possible to stagger the time response of each path such that each response occurs at the correct point in time. The sum of the echo path response for each point in time will lead to the total time response of the system of layers.

3.5 Implementation Validation

This section will provide evidence that the implementation of the Thompson-Gray model and the accompanying modifications accurately describe the ultrasonic response as generated by the armor.

3.5.1 Phase Validation

While the Transfer Matrix method may not be suitable for attaining the stated goals, it has great utility as a means for determining the accuracy of the phase calculations. This method

was derived in such a way that all possible echo paths for a set of layers are modeled, as mentioned in [section 2.2](#). The program used was written by Dr. Anxiang Li with the methods of data entry modified by the author and can be found in [Appendix E](#).

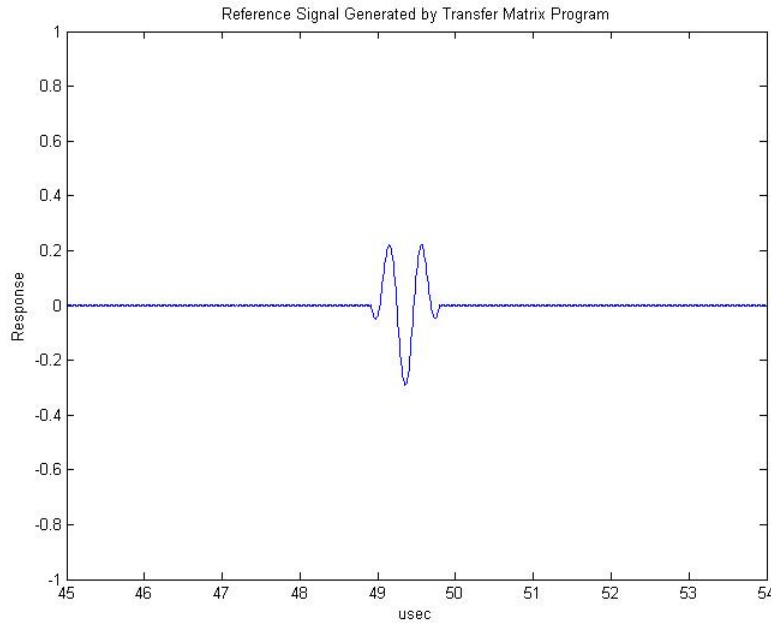


Figure 3.5 Transfer Matrix Generated Reference Signal - The signal above was created by the Transfer Matrix program by selecting zero gain. This will generate a simulated reference signal of the setup found in [Figure 2.3](#).

The first step in validation was to use the Transfer Matrix program to create a reference signal, [Figure 3.5](#), for use by the MLP. In this way, the same pulse used by the Transfer Matrix will be used by the MLP. From here the full echo path as calculated by the Echo Path Constructor, [section C.2](#). The armor layer configuration is used by MLP with the reference signal from the Transfer Matrix program to generate the simulated response for an undamaged layer. The Transfer Matrix program is then executed for the same layer configuration. The resulting responses show agreement of the time delay and the echo paths for the period of interest as seen by [Figure 3.6](#).

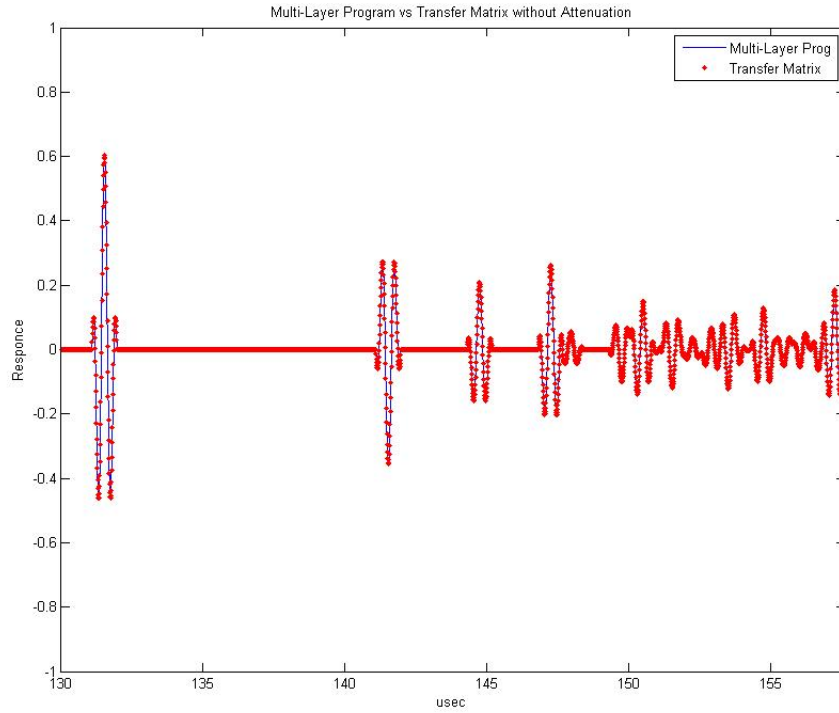


Figure 3.6 Phase Validation: The comparison shows excellent agreement between programs for phase and echo paths. The selected gain for the two compared response signals was zero.

3.5.2 Equivalent Path Collision Validation

To validate the necessity of using equivalent path collisions the Transfer Matrix program will be used to model an imaginary set of materials as seen in [Table 3.4](#). From theory, the Transfer Matrix would always account for both halves of any equivalent path collisions.

The collision being modeled arises from the paths 0 1 2 3 2 1 2 1 0 and 0 1 2 1 2 3 2 1 0. Modeling both paths is referred to as a collision and modeling only one of the pair is without a collision.

The Transfer Matrix program was run once for the above materials and MLP was run twice; once with the collision present and the other without the collision. This was achieved by removing the response from echo path 0 1 2 1 2 3 2 1 0.

As seen in [Figure 3.7](#), the signal with the full collision and the signal from the Transfer

Material	Thickness(cm)	Velocity(cm/ μ s)	Density(g/cm ³)	C (Nepers/cm)	p
Water	9.7	0.148	1	0.000275	2
Material A	1.0	0.4	1.5	0.000	1
Material B	1.7	0.4	2.25	0.000	1
Water	9.7	0.18	1	0.000275	2

Table 3.4 The material properties for these layers were selected to ensure that there is no overlapping of the signals so that any difference in amplitude because of collisions can be seen. Layers are in order as though for calculation.

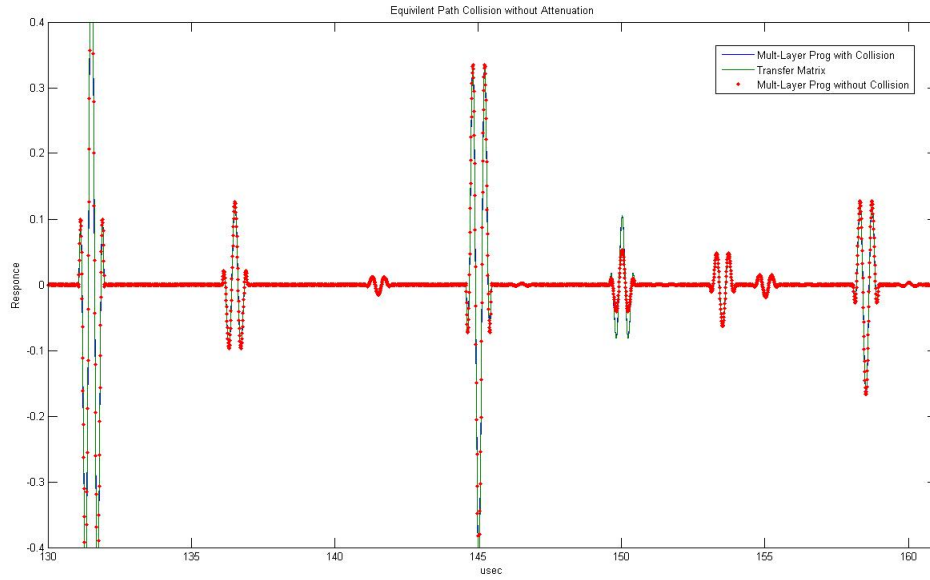


Figure 3.7 The collision of interest occurs at approximately 150 μ s.

Matrix program completely agree and the signal with only half of a collision is at half the amplitude for the specified signals.

3.5.3 Attenuation and Diffraction Validation

To validate attenuation and diffraction implementation the response generated by MLP is compared to experimentally collected signal from armor sample for both the flawed and unflawed cases with inspections occurring through the fiberglass side.

The pulse-echo inspection was conducted by first normalizing the probe to the inspection

surface and ensuring that the scanning direction is parallel to the inspection surface. A water path of approximately 9.6 cm and 2.36 cm was used for the inspection through the fiberglass and carbon fibers surfaces respectively.

There is a detectable amount of variation in the compaction of the layers resulting in small time shifts of the response between the layers of different panels. To ensure the comparison between MLP and the experimental response is not skewed by this variation a few experimental signals were shifted in time to align the experimental data more closely to one another. The MLP used the reference signal as seen in [Figure 2.4](#) to compute the following results and the difference in gain between the experimental signals and the reference signal is 22 dB.

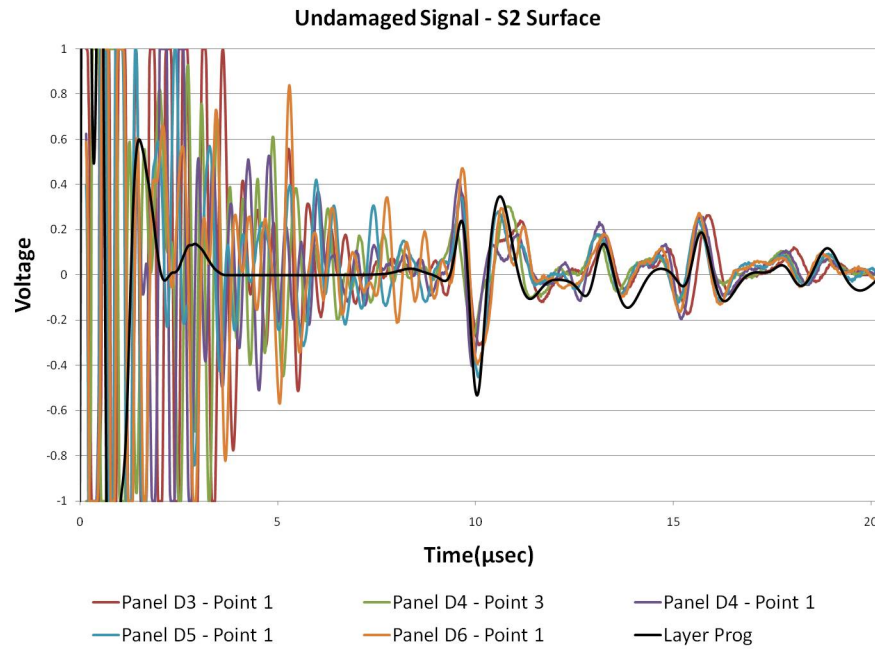


Figure 3.8 Comparison between experimental data of an undamaged armor panel and MLP results.

The damaged panels have artificial defects made of a Kapton pillow placed along some interfaces. The defect is modeled in MLP by a 0.05cm thick layer of air inserted between the specified layers.

From [Figure 3.8](#)–[Figure 3.10](#) it is evident that there is agreement between MLP and the experimental results. From this, the functionality of MLP for determining attenuation and

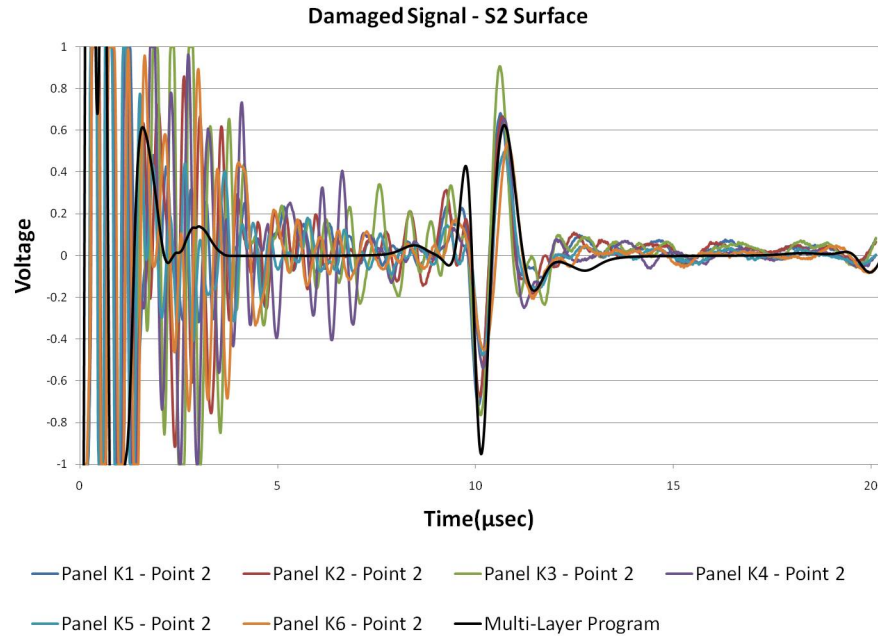


Figure 3.9 Comparison between experimental data of a damaged armor panel and MLP results. The delamination is located along the fiberglass-rubber interface.

diffraction is confirmed.

3.6 Inspection through Carbon Fiber Surface

The experimental data that was taken through the carbon fiber surface shows only minor difference in amplitude between the flawed and unflawed panels as seen in [Figure 3.11](#) and [Figure 3.12](#). The difference in gain between the reference signal and the experimental signal is 12 dB. This is the value used for the gain in the model.

It can be seen that there is very little difference between the signals. The MLP shows a slight increase in response around $8.5 \mu\text{sec}$ however that discrepancy will be explained. The lack of defect response is due to the inspection plan not being designed for inspection through this surface.

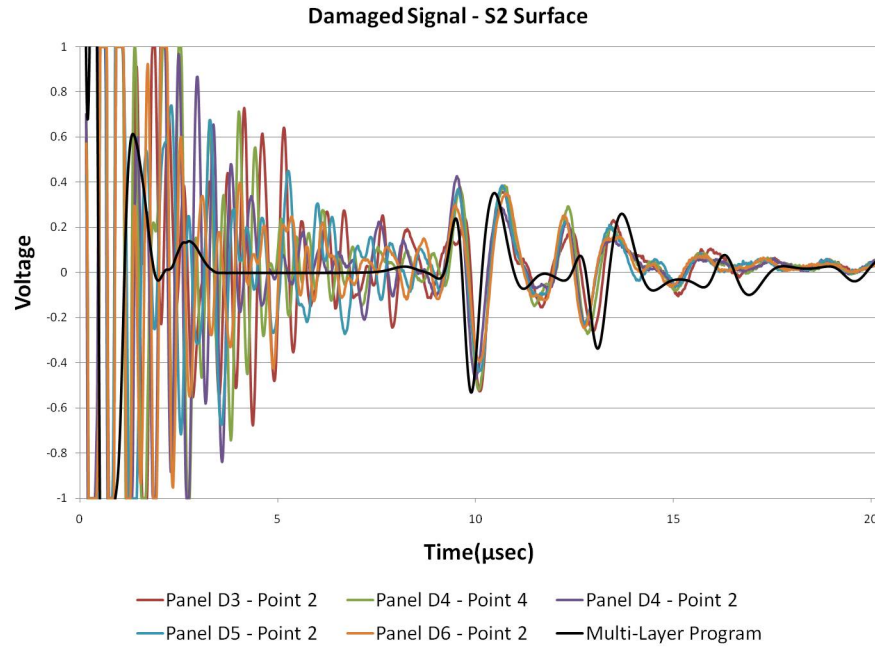


Figure 3.10 Comparison between experimental data of a damaged armor panel and MLP results. The delamination is located along the rubber-carbon fiber interface.

3.6.1 Inspection Plan Deficiencies

There exist two main deficiencies of the inspection plan used for the carbon fiber side. The first deficiency is that the focal length of the transducer is not long enough to reach the interface of the defect. This may reduce the amplitude of the reflection to below a detectable level. The second deficiency arises from the low inspection frequency. A 2.25 MHz transducer was required to inspect through the highly attenuative fiberglass layer. The long pulse length is detrimental to the inspection of thinner less attenuative layers where it will cause significant signal overlap.

3.6.2 Inspection Plan Development

In order to determine a more suitable scanning plan several situations will be considered. Investigation of the effects of changes in focal length as well as frequency will take place. The transducers will be modeled by physical properties as denoted in [Table 3.5](#) and the pulses as

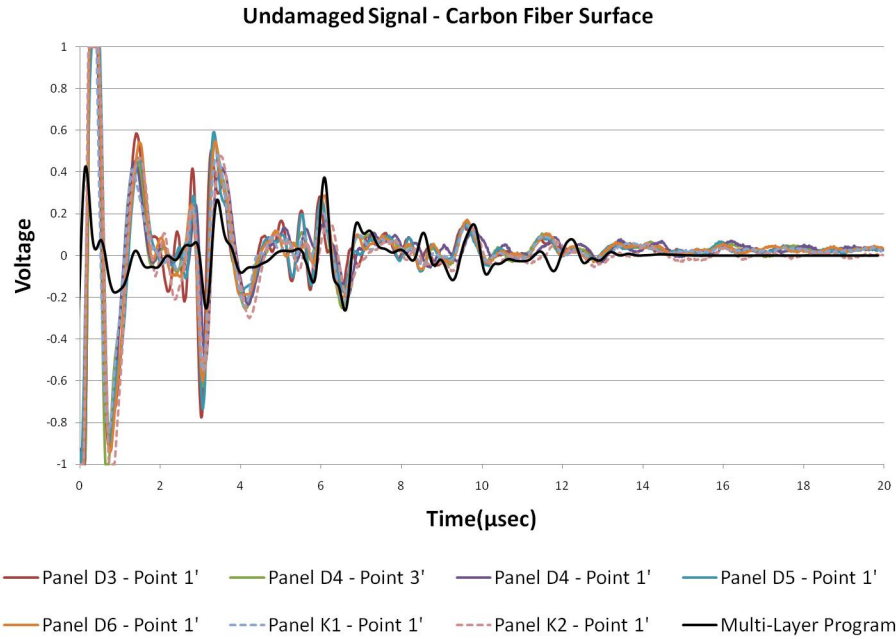


Figure 3.11 The undamaged pulse-echo signal taken from the carbon fiber side. These inspections had a 2.36 cm thick water layer.

seen in [Figure 3.14](#) and [Figure 3.15](#). For a proper comparison, the diffraction correction for the reference must be comparable between the different focal lengths. To accomplish this, the thickness of the fused quartz layer in the reference is adjusted such that, regardless of the focal length, the transducer focal plane is at the far interface.

Transducer	Effective Diameter	Geometric Focal Length
A	1.50 in.	7.5 in.
B	1.50 in.	8.5 in.
C	1.50 in.	9.5 in.

Table 3.5 The physical specifications for the MLP of the modeled transducers. These physical characteristics will be used for 2.25 MHz, 5 MHz, and 10 MHz cases.

Eighteen simulations will be compared; each of the three transducers operating at 2.25 MHz, 5 MHz, and 10 MHz for the flawed and unflawed cases. The graphs of the model predictions are located in [chapter 4](#). The geometric focal lengths in water were selected throughout the use of the equivalent layer thickness in water as seen in [Equation 3.7](#).

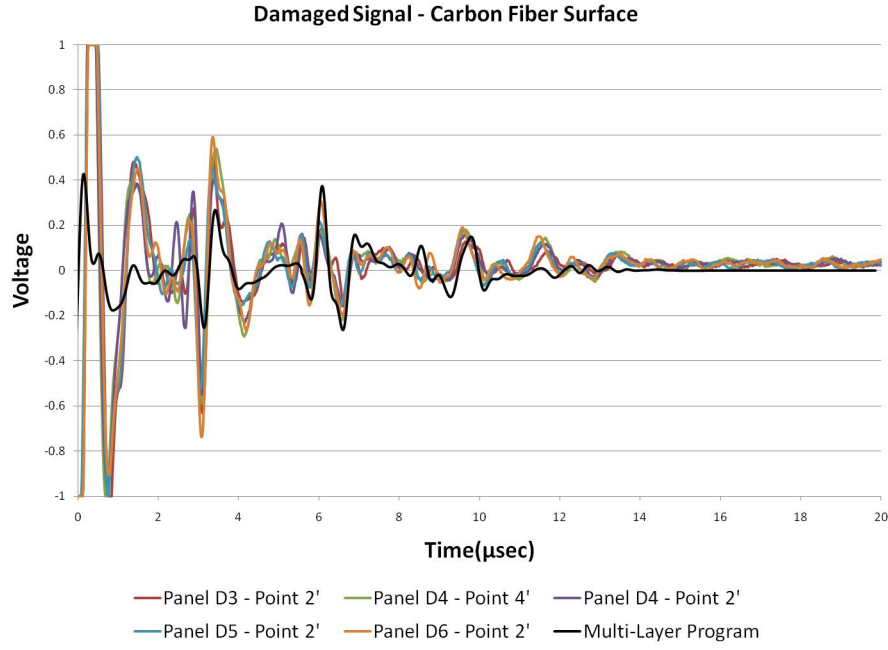


Figure 3.12 The damaged pulse-echo signal taken from the carbon fiber side. The artificial defects are along the rubber-carbon fiber interface.

$$F = \sum_{i=0}^N \frac{v_i}{v_0} z_i \quad (3.7)$$

Where F is the needed focal length to focus on the second interface of the N^{th} layer with i individually denoting the layer number with zero being the water layer.

The focal length of transducer B resided along the carbon fiber and rubber interface. The focal plane of transducer A is located inside the SiC ceramic layer and the focal plane for transducer C is located inside the S2 fiberglass layer.

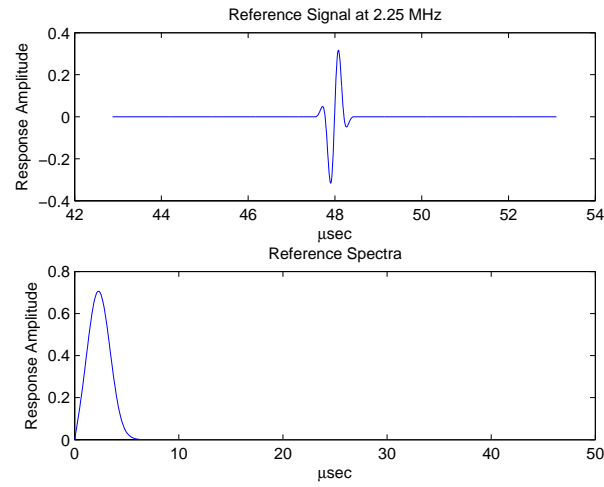


Figure 3.13 The 2.25 MHz reference signal and spectra as calculated with the Spike Generator program as located in [section C.4](#). This pulse has an absolute -3dB bandwidth of 1.9 MHz.

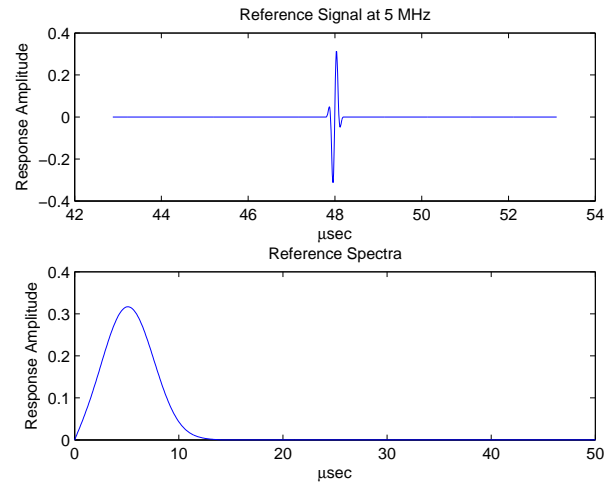


Figure 3.14 The 5 MHz reference signal and spectra as calculated with the Spike Generator program. This pulse has an absolute -3dB bandwidth of 4 MHz.

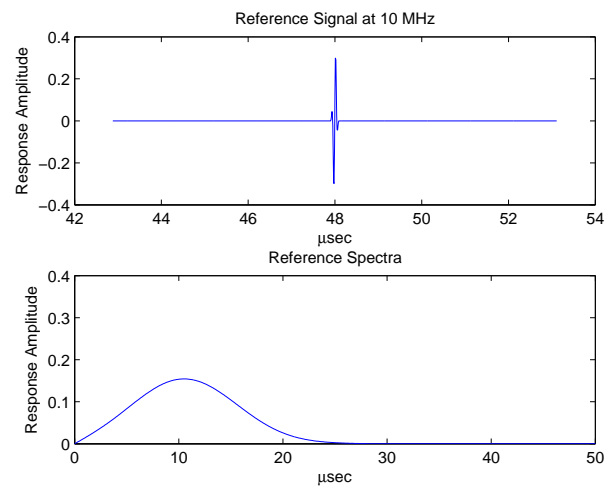


Figure 3.15 The 10 MHz reference signal and spectra as calculated with the Spike Generator program. This pulse has an absolute -3dB bandwidth of 8.4 MHz.

CHAPTER 4. RESULTS

In this chapter the Multi-Layer Program will be used to calculate the pulse-echo response through the carbon fiber face of an armor panel for cases as outlined in [subsection 3.6.2](#). All simulations are conducted with 10 dB of gain. For the flawed panels, the sole defect occurs along the carbon fiber-rubber interface at 41 μsec .

4.1 2.25 MHz Inspection Model

In this section the results of the three transducers for a 2.25 MHz inspection shall be presented.

4.1.1 Transducer A

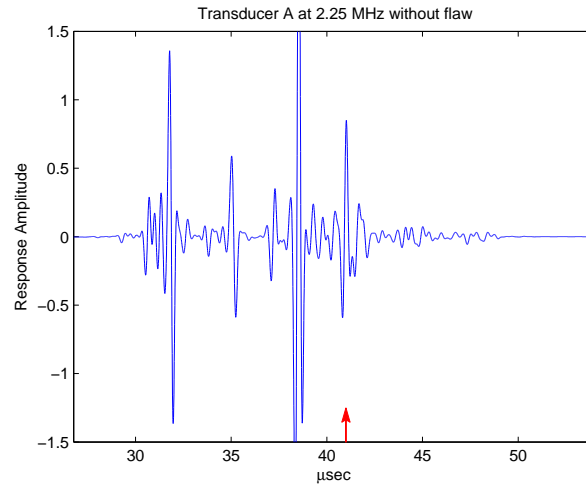


Figure 4.1 The simulated response of a 2.25 MHz transducer focused at the equivalent length of 7.5 in for the unflawed configuration.

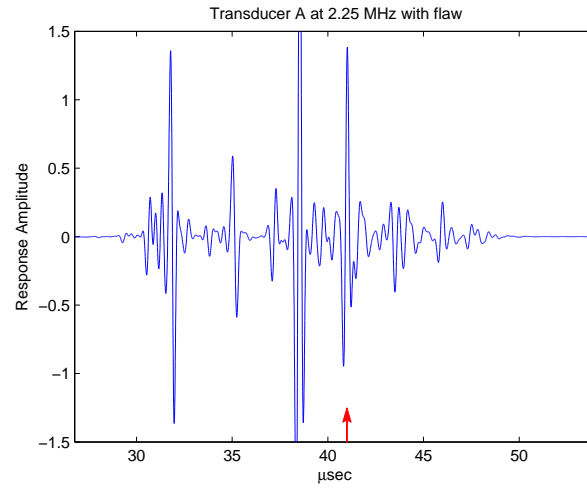


Figure 4.2 The simulated response of a 2.25 MHz transducer focused at the equivalent length of 7.5 in for the flawed configuration.

4.1.2 Transducer B

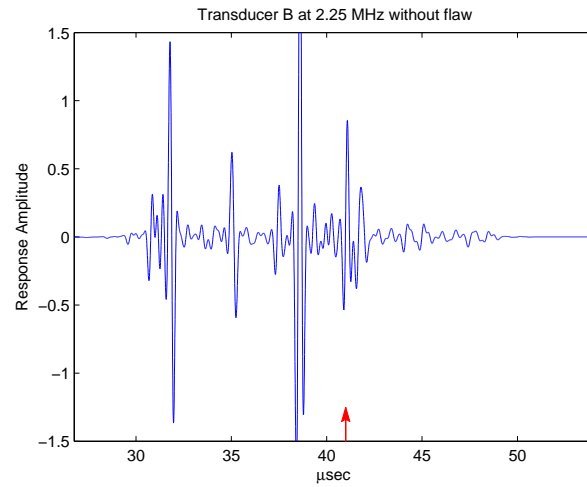


Figure 4.3 The simulated response of a 2.25 MHz transducer focused at the equivalent length of 8.5 in for the unflawed configuration.

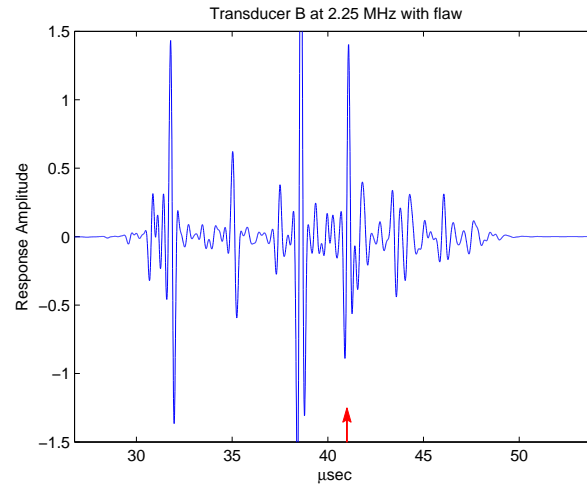


Figure 4.4 The simulated response of a 2.25 MHz transducer focused at the equivalent length of 8.5 in for the flawed configuration.

4.1.3 Transducer C

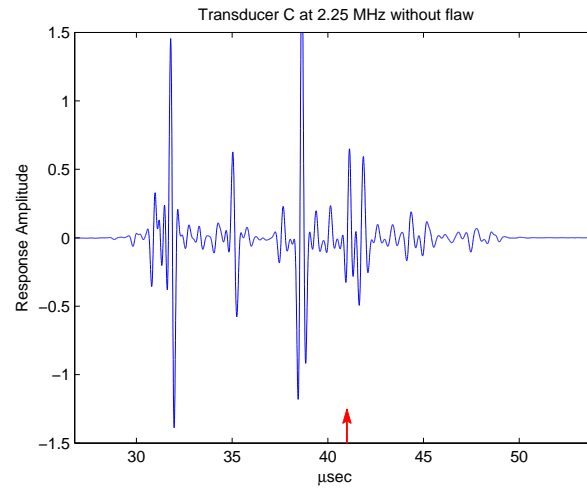


Figure 4.5 The simulated response of a 2.25 MHz transducer focused at the equivalent length of 9.5 in for the unflawed configuration.

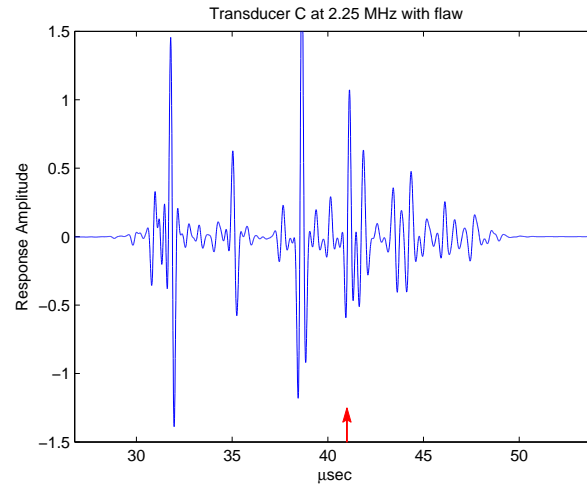


Figure 4.6 The simulated response of a 2.25 MHz transducer focused at the equivalent length of 9.5 in for the flawed configuration.

4.2 5 MHz Inspection Model

In this section the results of the three transducers for a 5 MHz inspection shall be presented.

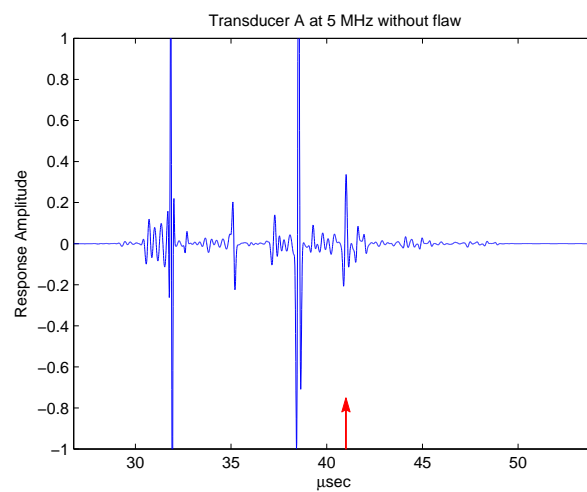


Figure 4.7 The simulated response of a 5 MHz transducer focused at the equivalent length of 7.5 in for the unflawed configuration.

4.2.1 Transducer A

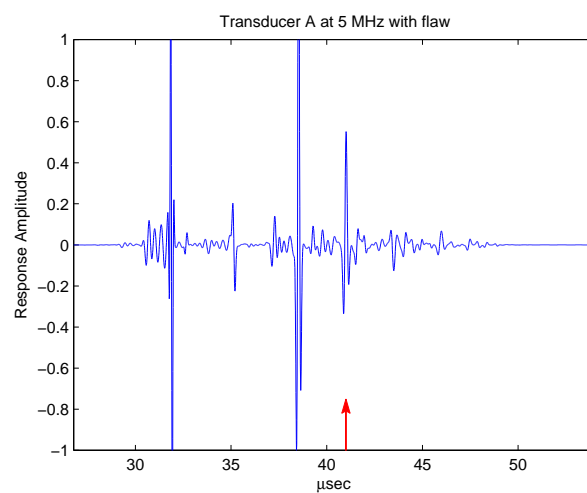


Figure 4.8 The simulated response of a 5 MHz transducer focused at the equivalent length of 7.5 in for the flawed configuration.

4.2.2 Transducer B

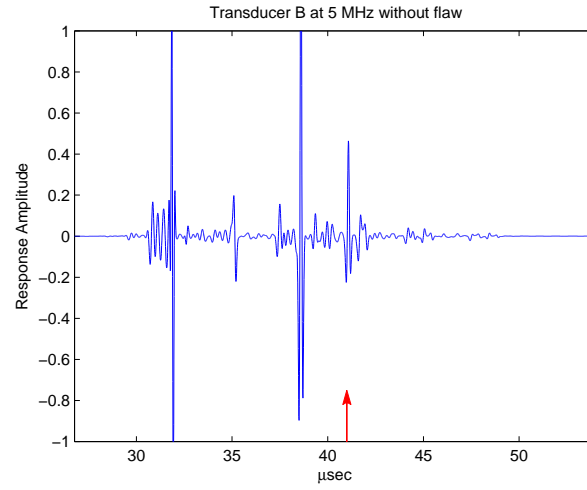


Figure 4.9 The simulated response of a 5 MHz transducer focused at the equivalent length of 8.5 in for the unflawed configuration.

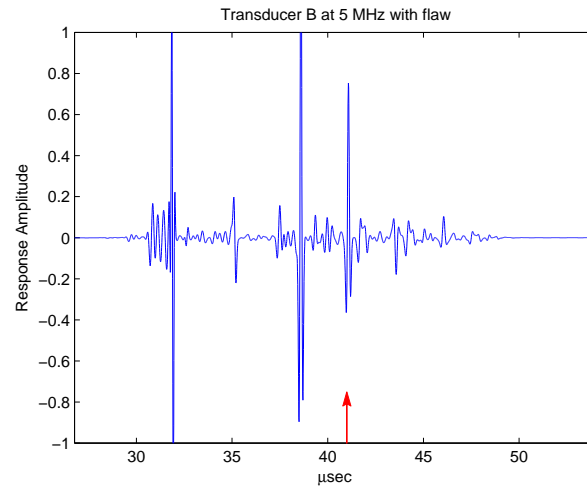


Figure 4.10 The simulated response of a 5 MHz transducer focused at the equivalent length of 8.5 in for the flawed configuration.

4.2.3 Transducer C

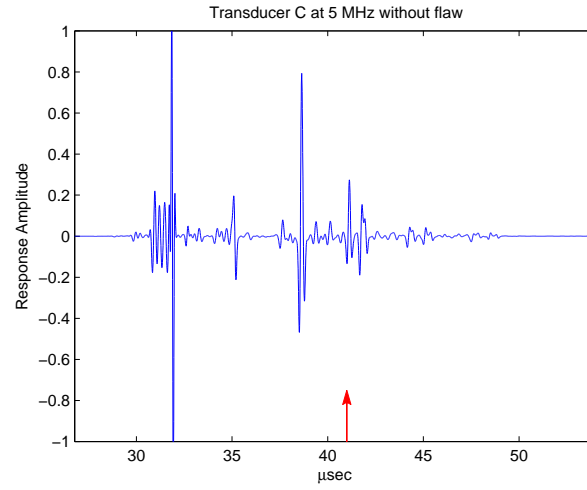


Figure 4.11 The simulated response of a 5 MHz transducer focused at the equivalent length of 9.5 in for the unflawed configuration.

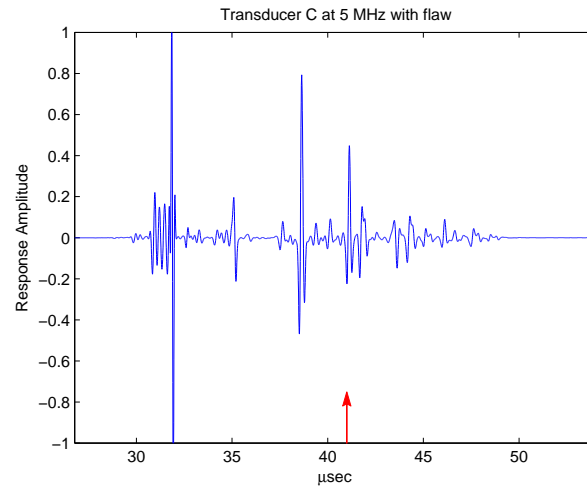


Figure 4.12 The simulated response of a 5 MHz transducer focused at the equivalent length of 9.5 in for the flawed configuration.

4.3 10 MHz Inspection Model

In this section the resulting simulations of the three transducers for a 10 MHz inspection shall be presented.

4.3.1 Transducer A

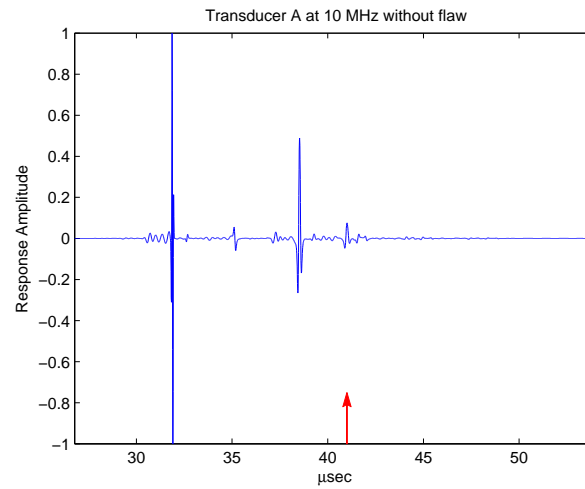


Figure 4.13 The simulated response of a 10 MHz transducer focused at the equivalent length of 7.5 in for the unflawed configuration.

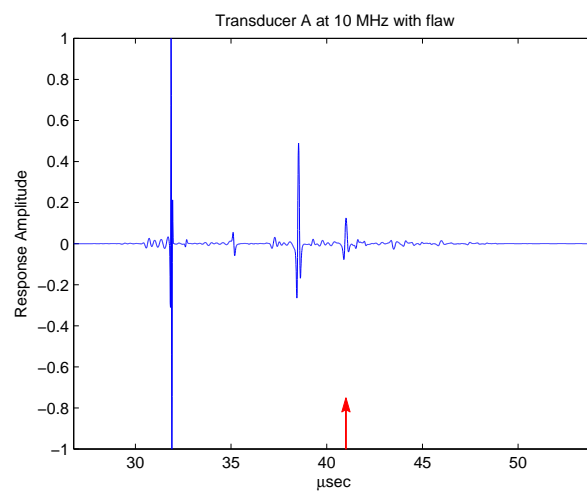


Figure 4.14 The simulated response of a 10 MHz transducer focused at the equivalent length of 7.5 in for the flawed configuration.

4.3.2 Transducer B

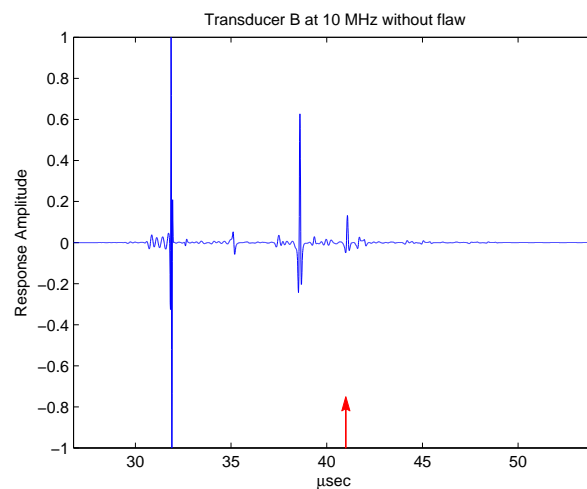


Figure 4.15 The simulated response of a 10 MHz transducer focused at the equivalent length of 8.5 in for the unflawed configuration.

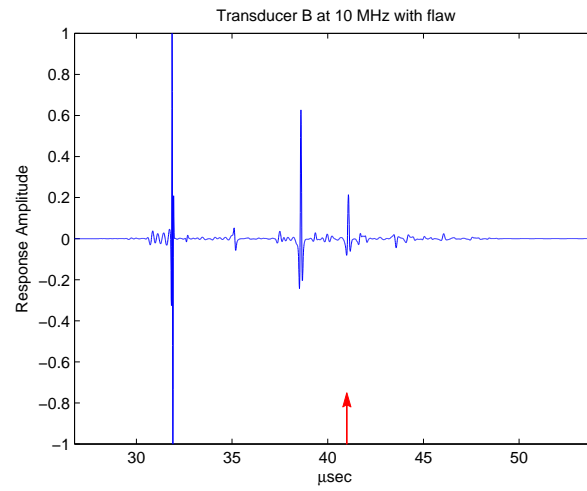


Figure 4.16 The simulated response of a 10 MHz transducer focused at the equivalent length of 8.5 in for the flawed configuration.

4.3.3 Transducer C

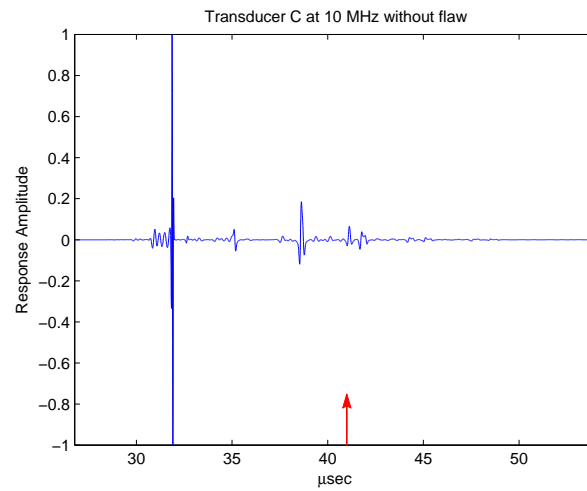


Figure 4.17 The simulated response of a 10 MHz transducer focused at the equivalent length of 9.5 in for the unflawed configuration.

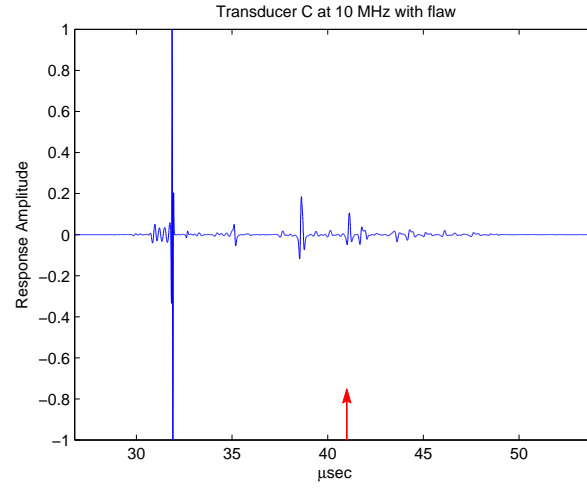


Figure 4.18 The simulated response of a 10 MHz transducer focused at the equivalent length of 9.5 in for the flawed configuration.

4.4 Flaw Amplitudes

This section contains tabulated and graphed information concerning flaw amplitude and response ratios.

Focal Length	2.25 MHz	5 MHz	10 MHz
7.5	1.38489	0.55178	0.12474
8.5	1.40268	0.75270	0.21425
9.5	1.07173	0.44836	0.10637

Table 4.1 The flaw amplitude values tabulated by focal length and frequency.

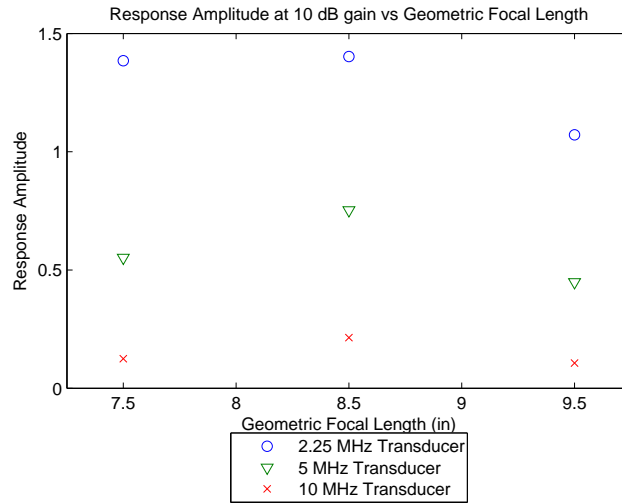


Figure 4.19 Amplitude versus focal length for a flaw located along the carbon fiber and rubber interface at three frequencies.

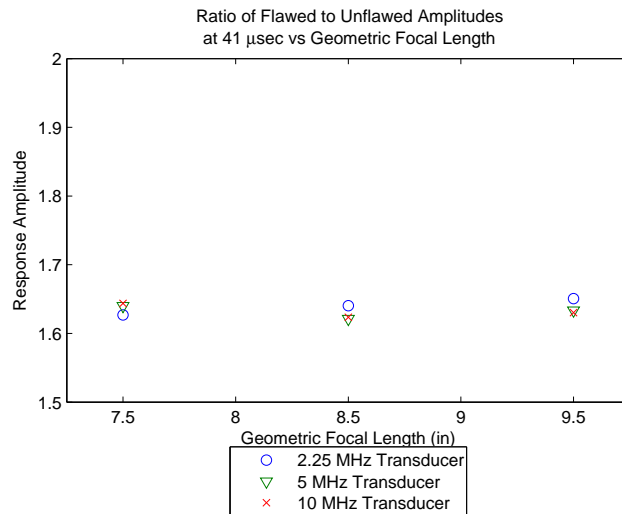


Figure 4.20 Flawed to Unflawed Ratio versus focal length for a flaw located along the carbon fiber and rubber interface at three frequencies.

CHAPTER 5. DISCUSSION

In this chapter the comparison of the experimental data and the model results, [subsection 3.5.3](#) and [section 3.6](#) will be discussed more deeply and the data presented in [chapter 4](#) shall be critically review to determine the best combination of frequency and focal length.

5.1 Experimental Data and the Model

While there is agreement of the model to the experimental data, there are regions of the experimental signal that are artifacts of the model derivation and need to be discussed.

5.1.1 Lack of Compaction

The first artifact is found in the figures of [subsection 3.5.3](#). In the first 9 μsec of the signal, thickness of the fiberglass layer, there is a significant amount of noise present in the experimental signals. Visual examination of a material specimen shows a severe lack of compaction that will cause the layer to be highly inhomogeneous and high surface roughness. Both will contribute to the noise levels but the inhomogeneity is the major component because the lack of compaction is so severe that the fiberglass layer may be more accurately modeled by several thinner layers of the same material. The model as formulated, however, assumes that all layers are homogeneous. The inclusion of inhomogeneous effects will aid in the accurate representation of the fiberglass layer. A separate method for the modeling of anisotropic effects needs would also increase the reliability of the model. These could be a topics of future work.

5.1.2 Adhesive Layer

The next artifact involves the effect of adhesive on the interfaces. While the time delay of the interfaces can be considered by increasing, the layer thickness of the composite layers slightly this does nothing to model the effects of attenuation on amplitude.

5.1.3 Defect Size

The last artifact is in [Figure 3.11](#) and [Figure 3.12](#). Shortly after 8 μsec there is a small but noticeable increase in amplitude that is not evident in either experimental signal. This is a result in a discrepancy between the model and the layer properties. In the model adhesive properties are modeled by the increasing the size of the composite layer slightly, but in the actual panel the adhesive at that layer must have a lower reflection coefficient than the carbon fiber-rubber interface.

5.2 Inspection Plan Motivated by Simulations

This section is dedicated to the development of an inspection plan through the carbon fiber surface.

5.2.1 Comparison of Signal Amplitudes

For the detection of the defect along and interface, the signal must be larger than the signal interface to be easily detectable. The ratio of the defect signal and the interface signal is displayed in [Figure 4.20](#). From the figure, it can be seen that the signal to noise ratio is approximately equivalent across frequency and focal length. This implies that all configurations are equally suitable for discerning the signal of the flaw from the unflawed interface.

5.2.2 Frequency

The graphs of the full response in [chapter 4](#) and, specifically, the flaw amplitude table and graph in [section 4.4](#) show that the amplitudes of the 2.25 MHz case are much greater than the amplitudes at 5 MHz or 10 MHz. A simple analysis of the 5 MHz and 10 MHz signals for

the reflection from the defect, at 41 μsec , reveals that the defect signal has a major frequency component of approximately 3 MHz. This is due to the attenuation of the carbon fiber layers. This explains the higher amplitudes for the 2.25 MHz transducer because there will be less amplitude loss from attenuation at the central frequency. Despite the higher amplitude, there is a noticeable decrease in temporal resolution for the 2.25 MHz frequency.

5.2.3 Focal Length

The table and graph of flaw amplitudes in [section 4.4](#) illustrates that as the focal length approaches the effective layer thickness of the interface so too does the amplitude of the response. As expected, the amplitude reaches a maximum when the focal length matched the equivalent thickness of the defect interface and decreases as the focal plane moves away from that interface. This is illustrated in [Figure 4.19](#) and [Table 4.1](#).

CHAPTER 6. CONCLUSION

This section reviews the development, validation, and utilization of the model developed in this thesis.

The inspection model as described in this thesis is developed for use with multiple parallel layers and is an extension of the model developed by [Thompson and Gray \(1983b\)](#). This was accomplished in a large part through two actions. The first assumption was that the beam size is smaller than the flaw. This allowed the use of a simpler model that only involves the diffraction and reflection terms, [Equation 2.8](#). The second was the description of multiple layers using reflection and transmission coefficients and equivalent material thickness. In order to describe multiple layers the product of the reflection and transmission coefficients for each echo path were required with the total signal being a composite of the individual paths at each point in time. To calculate the diffraction coefficient for multiple layers the equivalent layer thickness is used to describe multiple layers as a single layer of material.

These components were validated experimentally and excellent agreement is demonstrated in [section 3.5](#). The phase was validated using the Transfer Matrix method and the attenuation and diffraction components are validated by agreement with experimental signals both with and without a flaw.

To improve agreement further, efforts could be made to model the effects of anisotropy of the layer materials and to include adhesive material properties. While many materials are anisotropic, this model assumes isotropy. Anisotropy could be implemented by applying a method similar to the one as outlined in [Minachi et al. \(1993\)](#), where the anisotropy is modeled through a Taylor series expansion of the slowness vector. In order to implement this method directly one would need to evaluate the diffraction for each layer of an echo path rather than

as a single layer of equivalent thickness in water.

To model an adhesive layer two components would need further consideration. The first component is the consideration of the effect of the adhesive on signal amplitude. The second component is the consideration of the time delay caused by the adhesive. Two limiting conditions should be investigated further to aid in such modifications. The first is when the adhesive thickness is much smaller than the neighboring layers and the adhesive layer is smaller than a single wavelength. The second is when the adhesive layer thickness is greater than a single wavelength.

The model was then used to investigate the response of a flaw at constant depth while varying frequency and focal length in [chapter 5](#). Of the focal lengths, 7.5, 8.5, and 9.5 inches in water, the focal length of 8.5 inches resulted in the highest amplitude across all three frequencies. This is supported by theory because the focal length of 8.5 inches places the focal point at the flaw interface where the least phase cancelations will occur. Out of the three frequencies, 2.25 MHz produced the highest responses at the expense of resolution. As such, a center frequency of 2.25 would be preferable if this inspection were to confine its scope to defects along the layer boundaries. If defects can occur on the interior of the layer, such as if they were damaged through combat or from shipping, then a higher frequency would be recommended to allow for the resolution of the flaw from the interface response.

In conclusion, the model proved able to predict the response of the armor panels for both flawed and unflawed cases. It is shown that for inspections along the layer boundaries and the interior of the layer the model can be used successfully to determine the nominal focal length and frequency of a transducer. This model aided in the inspection of over 36 armor specimens of varying defect configuration by allowing for the rapid development of inspection plans. This model will continue to be utilized to model the response of alternative armor configurations.

BIBLIOGRAPHY

- ASTME494-05 (2005). *Standard Practice for Measuring Ultrasonic Velocity in Materials*. American Society for Testing Materials International, West Conshohocken, PA.
- Cheeseman, B. A., Jensen, R., and Hoppel, C. (2004). Protecting the future force: Advanced materials and analysis enable robust composite armor. *AMPTIAC Quarterly*, 8(4):37–72.
- Cooley, J. W. and Tukey, J. W. (1965). An algorithm for the machine calculation of complex fourier series. *Math. Comp.*, 19:297–301.
- Frigo, M. and Johnson, S. G. (2005). The design and implementation of FFTW3. *Proceedings of the IEEE*, 93(2):216–231. Special issue on “Program Generation, Optimization, and Platform Adaptation”.
- Margetan, F. J. and Thompson, R. B. (1994). Technical Report 5, ISU/ETC.
- Minachi, A., Margetan, F. J., and Hsu, D. K. (1993). Delamination sizing in composite materials using a gauss–hermite beam model. *Ultrasonics*, 31(4):237 – 243.
- Minachi, A., Margetan, F. J., and Thompson, R. B. (1998). Reconstruction of a piston transducer beam using multi-gaussian beams and its application. In *Review of Progress in Quantitative Nondestructive Evaluation*, pages 907–914.
- Panetta, P. D., Margetan, F. J., Yalda, I., and Thompson, R. B. (1995). Ultrasonic attenuation measurements in jet-engine titanium alloys. In *Review of Progress in Quantitative Nondestructive Evaluation*, pages 1525–1532.
- Thompson, R. B. and Gray, T. A. (1981). Range of applicability of inversion algorithms. In *Review of Progress in Quantitative Nondestructive Evaluation*, page 233.

- Thompson, R. B. and Gray, T. A. (1983a). Analytic diffraction corrections to ultrasonic scattering measurements. In *Review of Progress in Quantitative Nondestructive Evaluation*, page 567.
- Thompson, R. B. and Gray, T. A. (1983b). A model relating ultrasonic scattering measurements through liquid–solid interfaces to unbounded medium scattering amplitudes. *The Journal of the Acoustical Society of America*, 74(4):1279–1290.
- Thomson, W. T. (1950). Transmission of elastic waves through a stratified solid medium. *Journal of Applied Physics*, 21(2):89–93.

APPENDIX A. GEOMETRIC FOCAL LENGTH AND EFFECTIVE DIAMETER DATA

A.1 Transducer Spectra

The spectra measurements were taken at a distance z from the target that the amplitude of the waveform was maximized.

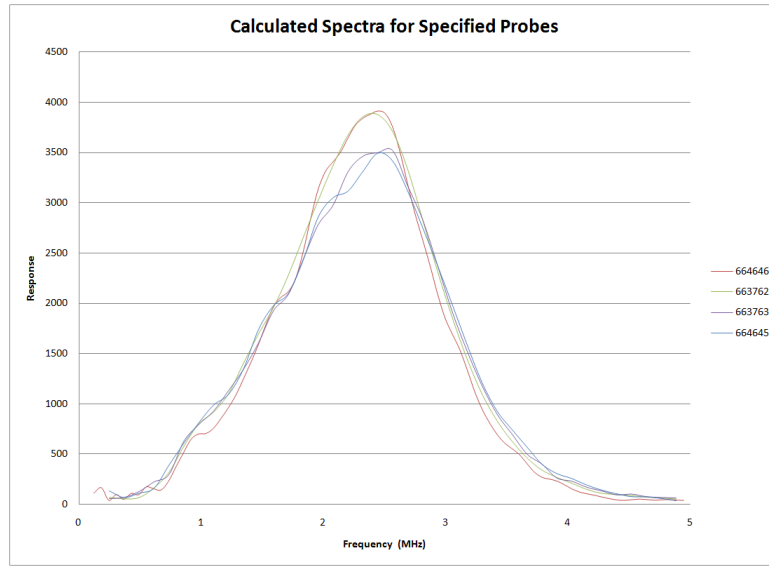


Figure A.1 Spectra for the probes: 663762, 663763, 664645, and 664646 with gains of 12, 16, 26, and 27 dB respectively.

A.2 Effective Diameter and Geometric Focal Length as a function of diameter.

The constant effective diameter listed in the figures of this appendix are the values arrived at from the average of a weighted combination fit over ranges of frequencies for both the focal

length and diameter.

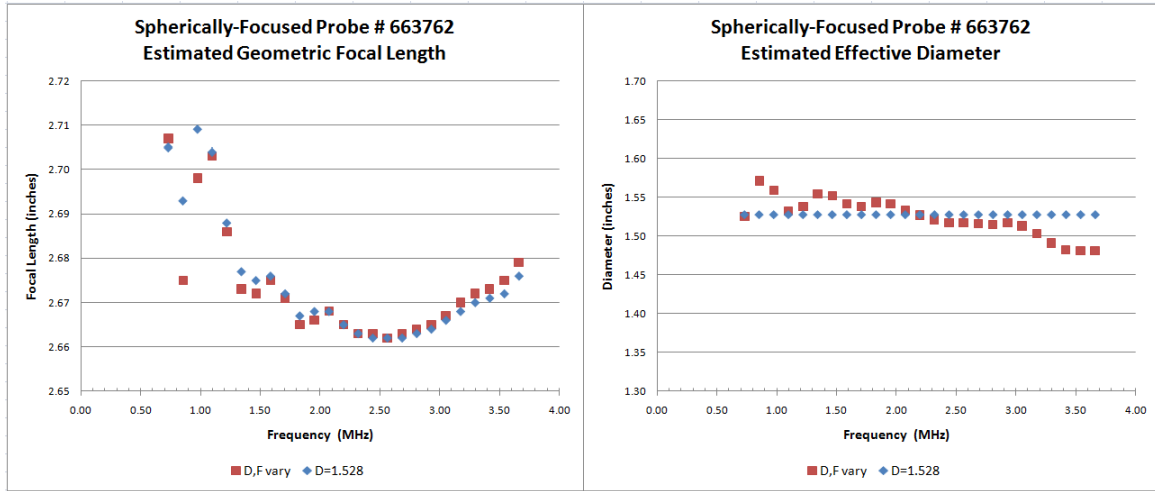


Figure A.2 Geometric Focal Length and Effective Diameter as a Function of Frequency for Transducer 663762

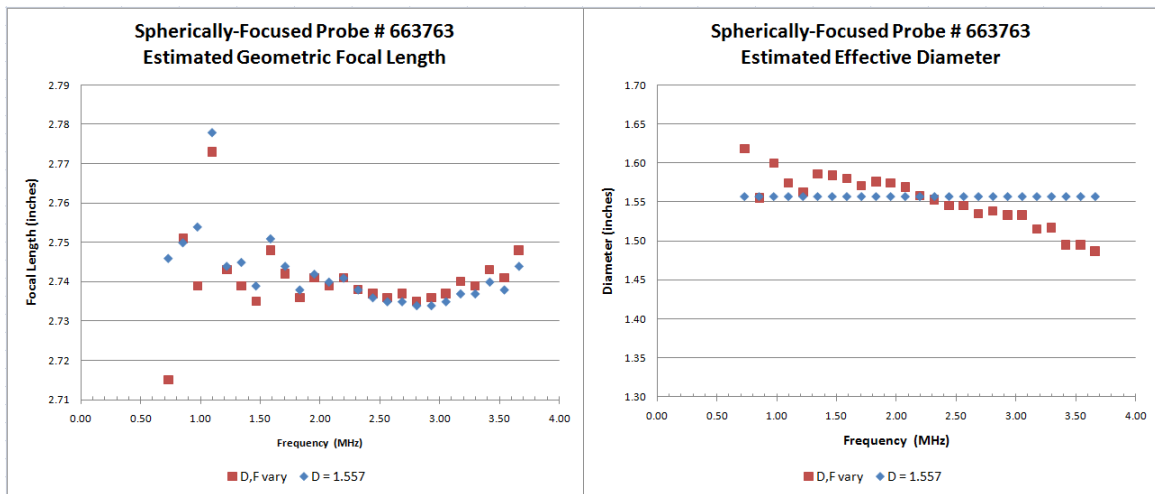


Figure A.3 Geometric Focal Length and Effective Diameter as a Function of Frequency for Transducer 663763

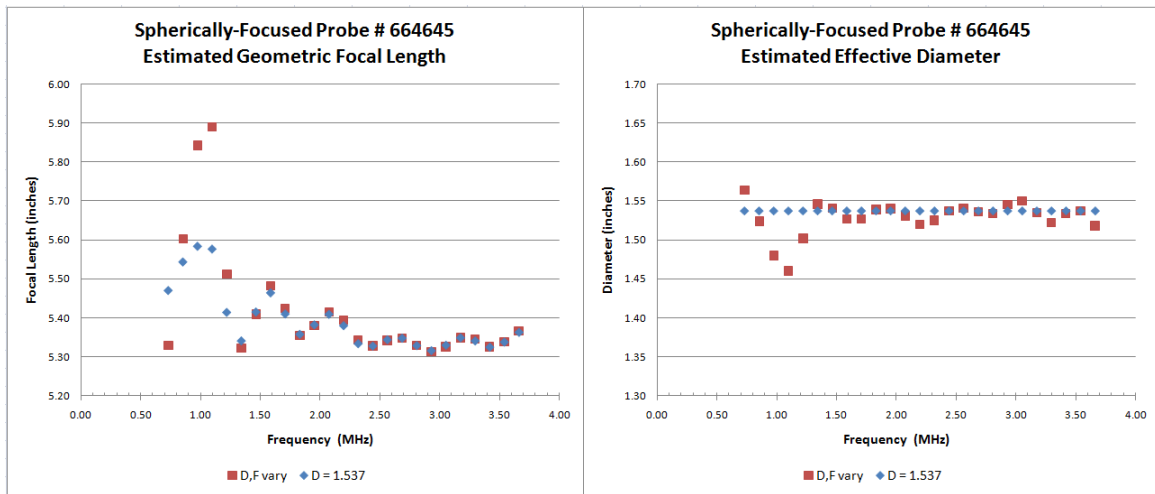


Figure A.4 Geometric Focal Length and Effective Diameter as a Function of Frequency for Transducer 664645

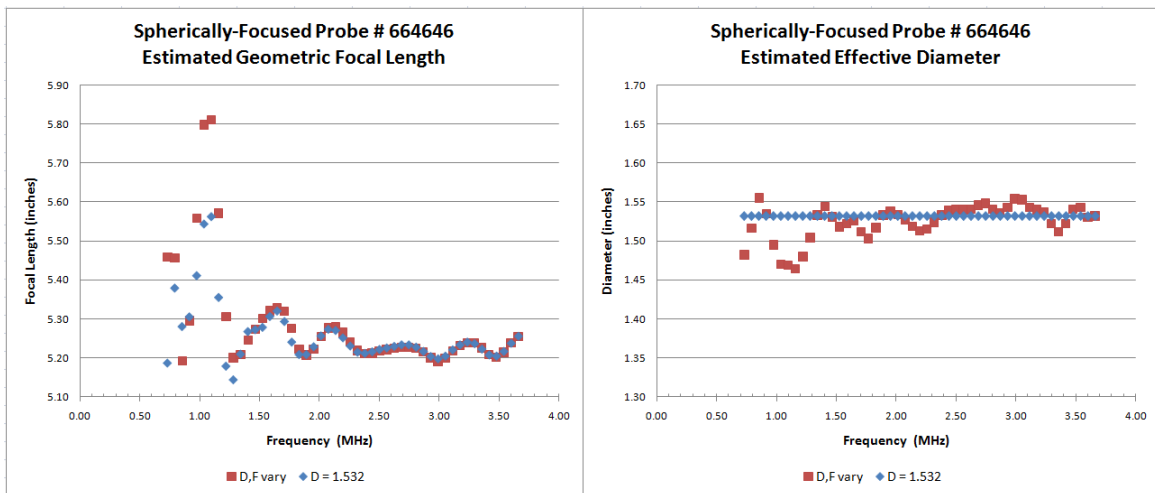


Figure A.5 Geometric Focal Length and Effective Diameter as a Function of Frequency for Transducer 664646

APPENDIX B. ATTENUATION COEFFICIENT MEASUREMENTS

This program measures the attenuation from an unknown material through comparison with a known reference material.

```

%% Load/Average Data and Load Properties
clear all;close all
type=input('Was this a through transmission measurment?(Y/N) ','s');
if type == 'Y'
    disp('NOTE: It is assumed that a planar probe is the transmitter while a
        focused probe is the reciver.')
    freq=input('What is its nominal center frequency?(MHz)');
end
WPR=input('What is the waterpath between the sample and the receiver?(cm)');
temp=input('What was water temperature?(deg C)');
backup=input('Was the water path adjusted for reference measurment?(Y/N) ','s');
dB=input('What is the difference in dB between the material signal and reference?'
    );
l=input('How many files do you wish to load?');
disp('*****LOAD REFERENCE SIGNAL LAST*****')
%%

%%%%%%%%%%%% User Defined %%%%%%%%%%%%%%
z1=0.03302;
v1=0.192;
rho1=0.97;
%%%%%%%%%%%%%%%%%%%%%%%%%%%%%%%%%%%%%%%%

```

```

v0=waterT_c(temp);

Z1=v1*rho1;
Z0=v0*1;
TT=4*Z0*Z1/(Z0+Z1)^2;

if backup == 'Y'
    WPA=(v1/v0*z1-z1);
else
    WPA=0;
end

fname= uigetfile('Z:\*.*','MultiSelect','on');
figure(1)
hold on
color=['b','r','g','m','c','y','k'];
for k=1:l
    [labels,t,v] = readColData(char(fname(k)),2);
    plot(t,v(:,1),color(k));
    if k==1
        N=2^nextpow2(length(v(:,1))*2);
        dt=t(2)-t(1);
        f(:,1)=s_space(0,1/dt,N);
    end
    if k<l
        F(:,k)=abs(FourierT(v(:,1),dt,N));
    else
        F_W(:,1)=abs(FourierT(v(:,1)*10^(dB/20),dt,N));
    end
end
end
%%
hold off
F(:,1)=sum(F,2)./(l-1);

figure(2); plot(f,F(:,1:l),f,F_W,'--')

```

```

axis([0 freq+5 0 max(F_W)])
legend('Site A','Site B','Site C','Site D','Site E','Site F','Average','Water')
title('Spectra')
xlabel('Frequency (MHz)')
ylabel('Response (arb)')

CF=input('What is the center frequency of probe?');
HBW=input('What is half the bandwidth?');

F_min=find(f>=(CF-HBW) & f<=(CF-HBW+0.15));
F_max=find(f>=(CF+HBW) & f<=(CF+HBW+0.1));
F_short(:,1)=F_W(F_min(1):F_max(1),1);
F_short(:,2:(l+1))=F(F_min(1):F_max(1),:);
f_short(:,1)=f(F_min(1):F_max(1),1);
%% Attenuation
syms a1 real

for j=1:l
    F_F(:,j)=F_short(:,j+1)./F_short(:,1);
    alphaH(:,j)=alpha_H2O(temp,f_short);
end

alpha=-(log(F_F/abs(TT))-alphaH*WPA)/(z1);

figure(3); plot(f_short(:,1),alpha(:,1:(l-1)),'Marker','.','LineStyle','none')
legend('Site A','Site B','Site C','Site D','Site E','Site F')
title('Attenuation of each Data Set')
xlabel('Frequency (MHz)')
ylabel('Attenuation (N/cm)')
figure(4); plot(f_short(:,1),alpha(:,l),'Marker','.','LineStyle','none')
title('Attenuation of Averaged Spectra')
xlabel('Frequency (MHz)')
ylabel('Attenuation (N/cm)')

uisave({'f_short','F_short','alpha'},'take');

```

APPENDIX C. COLLECTED PROGRAMS AND FUNCTIONS

In the following sections the source code of programs referenced and functions called by the main program are displayed. The programs below calculate the echo paths, reflection and transmission coefficients, diffraction correction, and the equivalent paths.

C.1 EQUIVALENT LAYER THICKNESS

This appendix contains the function for determining the equivalent layer path in terms of water.

```
function [echopath,TOFpath,layer]=eqvpath(ET,mat)

% This function calculates the number of times a signal passes through a
% layer. From this the equivalent waterpath of each echotrain is
% calculated.

layer=zeros(size(ET,1),size(mat,1)-1);

%Loop calculates the number of times path traverses layer
for k=1:size(ET,1)
    for n=2:ET(k,1)
        if ET(k,n)<ET(k,n+1)
            layer(k,ET(k,n+1))=layer(k,ET(k,n+1))+1;
        elseif ET(k,n)>ET(k,n+1)
            layer(k,ET(k,n))=layer(k,ET(k,n))+1;
        end
    end
end
```

```

        end
    end

    echopath=(mat(1,2).*(layer*(mat(1:6,1)./mat(1:6,2))))./2;
    %Equivilent thickness calculation
    TOFpath=2*echopath./mat(1,2);
    %Time of Flight calculation from equivilent thickness data

```

C.2 ECHO PATH CONSTRUCTOR

```

clear all
clc;
echotest=input('Is this an echo test?','s');
maxTOF=input('What is the max TOF?');
if echotest=='N'
    run data_frank
else
    mat= [9.70    0.148    1        0.000275    2;...    Layer 1
          1.00    0.4      1.5      0            1;...    Layer 2
          1.70    0.4      2.25    0            1;...    Layer 3
          9.70    0.148    1        0.000275    2];%    Layer 4
end

GC=input('Is the inspection occuring through the carbon fiber surface?(Y/N)','s');
if GC=='Y'
    mat=flipud(mat);
end

%% Raw Echo Path
test(1:1024,1:21)=NaN;
n=1:size(mat,1);

for i=1:1024

```

```

jprime=find(isnan(test(i,:))==0,1,'last')+1;
if isempty(jprime)==1
    jprime=1;
end
for j=jprime:21
    if i==1 && j==1
        test(i,j)=0;
    elseif i==1 && j==2
        test(i,j)=test(i,j-1)+1;
    elseif test(i,j-1)==0
        test(i,j)=test(i,j-1)+1;
    else
        ind=find(test(:,1)==0, 1, 'last' );
        test(ind+1,:)=test(i,:);
        test(ind+1,j)=test(i,j-1)+1;
        test(i,j)=test(i,j-1)-1;
        test(ind+2,:)=test(i,:);
        if rem(j,2)==1 && test(i,j)==0
            break
        end
    end
end
end
end

%% Clean Up - Remove Repitition & Consolidate List

ET(1:1024,1:21)=NaN;
n=0;
for i=1:1024
    n=0;
    for j=1:1024
        num=find(ET(j,:)==0,1,'last');
        if sum(test(i,:)==ET(j,:))==num &...
            num==find(test(i,:)==0,1,'last') |...
            sum(test(i,:)>size(mat,1)-1)>0

```

```

        n=n+1;
    end
end

if n==0
    ind=find(ET(:,1)==0, 1, 'last' );
    if isempty(ind)==1
        ind=0;
    end
    ET(ind+1,:)=test(i,:);
end
end

for i=1:length(ET)
    if isempty(find(ET(i,:)==0,1,'last'))==1
        break
    else
        num(i,1)=find(ET(i,:)==0,1,'last');
    end
end

test2=ET;
clear ET
et(1:length(num),1:22)=NaN;
et(:,1)=num;
et(:,2:22)=test2(1:length(num),:);
%%
n=1;
for i=1:length(et)
    [echopath,TOFpath,layer]=eqvpath(et(i,:),mat);
    if TOFpath < maxTOF
        ET(n,:)=et(i,:);
        n=n+1;
    end
end

sav=input('Save as...','s');

```



```
save(sav, 'ET')
```

C.3 REFLECTION AND TRANSMISSION FUNCTION

```
function RT=refl_tran(ET,mat)

%Determines impedance for all layers.
Z=mat(:,2).*mat(:,3);

%Determines reflection and transmission coefficients for all interfaces.
for m=1:(size(mat,1)-1)
    coeff(m,:)=[ (Z(m)-Z(m+1))/(Z(m)+Z(m+1))  2*Z(m)/(Z(m)+Z(m+1)) ...
                (Z(m+1)-Z(m))/(Z(m)+Z(m+1))  2*Z(m+1)/(Z(m)+Z(m+1)) ];
end

rt(1:size(ET,1),1:(max(ET(:,1))-2))=1;

%For a given echo path, i.e. 0 1 2 1 2 1 0, the loops below calculate
the needed reflection or transmission coefficients.

for k=1:size(ET,1)
    for n=1:(max(ET(k,2:size(ET,2))))
        for l=2:(ET(k,1)-1)
            if ET(k,l+2)-ET(k,l)==0 && ET(k,l+1)>ET(k,l)
                if ET(k,l+2)>ET(k,l+1)
                    rt(k,l-1)=coeff(ET(k,l+1),3);
                else
                    rt(k,l-1)=coeff(ET(k,l+1),1);
                end
            elseif ET(k,l+2)-ET(k,l)==0 && ET(k,l+1)<ET(k,l)
                if ET(k,l+2)>ET(k,l+1)
                    if ET(k,l+1)==0
```

```

        rt(k,l-1)=coeff(ET(k,l+1)+1,1);
    else
        rt(k,l-1)=coeff(ET(k,l+1),1);
    end
else
    rt(k,l-1)=coeff(ET(k,l+1),3);
end
elseif ET(k,l+1)-ET(k,l)==-1
    rt(k,l-1)=coeff(ET(k,l+1),4);
elseif ET(k,l+1)-ET(k,l)==1
    rt(k,l-1)=coeff(ET(k,l+1),2);
else
    end
end
end
end
end

RT=prod(rt,2);
%Determines the product of the coefficients for the path in question.

```

C.4 SPIKE GENERATOR

```

function T_FQ=spike_gen(N,dt,f0,TOF,p)
% TOF is the time of flight of the "reference" backwall measurement
% N is the number of points in reference waveform
% f0 is the center frequency of the probe
% dt is the inverse of the sampling rate
% p is 0 for no print and 1 for print.

ncycles=2;

pulsewidth = ncycles/f0; % duration of incident pulse

```

```

npulsewidth = pulsewidth/dt; % number of points in incident pulse
t0=linspace(0,pulsewidth,npulsewidth);

S(:,1)=sin(2*pi*f0*t0);
G(:,1)=normpdf(linspace(-3,3,npulsewidth),0,1);
spike(:,1)=padarray(S.*G, (N-length(t0))/2);
t=linspace((TOF-(N-length(t0)+npulsewidth)*dt/2), (TOF-(N-length(t0)+npulsewidth)*
    dt/2)+(N-1)*dt,N)';
T_FQ=[t spike];

if p==1
    df=1/(N*dt);
    f(:,1)=(1:N)'^-1*df;
    f_spike = fft(spike)*1/(dt*N);
    figure;subplot(2,1,1);plot(T_FQ(:,1),T_FQ(:,2))
    name=input('What is the desired title?','s');
    title(name)
    xlabel('\musec')
    ylabel('Response Amplitude')
    subplot(2,1,2);plot(f,abs(f_spike))
    name=input('What is the desired title?','s');
    title(name)
    xlabel('\musec')
    ylabel('Response Amplitude')
    axis([0 50 0 0.4])
    name=input('What is the desired filename?','s');
    set(gcf, 'PaperPositionMode','auto',...
        'PaperUnits', 'inches',...
        'PaperSize', [6 5]);
    print('-dpdf',name)
end

```

C.5 Diffraction Correction Call Function

This function provides the other diffraction functions, written by Dr. Margetan, with basic variables and calls them for calculations.

```
function D=diff_cor(V1,FREQ,Z1)

%%
%MODE=0 FOR A SINGLE GAUSSIAN;
%
%MODE=1 FOR THE WEN/BREAZEALE PISTON-PROBE EXPANSION USING 10 GAUSSIANS;
%
%MODE=2 FOR THE WEN/BREAZEALE PISTON-PROBE EXPANSIO USING 15 GAUSSIANS.

%MODE=input('Select the operation mode of the program(0,1,or2):');
MODE=1;
[ NG,AUNIT,BUNIT ] = MGREAD(MODE);

Z2=0;
V2=0;
B1X=1e20;
B1Y=B1X;
B2X=B1Y;
B2Y=B2X;
ITYPE=1;
FOCX=13.28;
FOCY=13.28;
AX=3.89/2;
AY=3.89/2;
%%
% Complex Beam Spread with using equivilent water path.
[ D ] = DMG(ITYPE,FOCX,FOCY,AX,AY,FREQ,V1,...
            V2,Z1,Z2,B1X,B1Y,B2X,B2Y,AUNIT,BUNIT,NG);
```

APPENDIX D. MULTI-LAYER PROGRAM

```

%% Layer Program
%
%%
clc
clear all
close all
entry_val='N';
entry_atten='N';
entry_diff='N';

run data_frank

loadorbuild=input('Do you wish to build your "reference" or load measured data?(0-
-> Build 1 --> Load)');

GC='Y';%input('Is the inspection occuring through the carbon fiber surface?(Y/N)
','s');
if GC=='Y'
    mat(size(mat,1):size(mat,1)+1,:)=[---- 0.336 1.78 0.6274 1.2117;...
        Fiberglass wrap
        9.70 0.148 1 0.000275 2];%Water layer

    mat=flipud(mat);
    mat(1,1)=2.36 ;
    mat(end,1)=2.36;
    clear ET
    load ET_GC

```

```

end

entry='N';%input('Enable debugging options?(Y/N) ','s');
if entry=='Y'
    entry_atten=input('Turn off attenuation?(Y/N) ','s');
    entry_diff=input('Turn off diffraction?(Y/N) ','s');
end

FL=input('What is the desired focal length?');
gain=input('What is the desired gain?');

if loadorbuid==0
    f0=input('What is the desired central frequency?');
    N=1024;%input('How many points should the reference signal hold?');

    z1_fq=(FL-z0)/(v1_fq/v0);
    ref_mat=[z0      v0      rho0      0.000275      2;...
             z1_fq  v1_fq  rho1_fq      0      1;...
             z0      v0      rho0      0.000275      2];

    [ref_eqv,TOF_ref,ref_layer]=eqvpath(ref_ET(2,:),ref_mat);

    dt=0.01;
    T_FQ=spike_gen(N,dt,f0,TOF_ref,0);
elseif loadorbuid==1
    fname= uigetfile('C:\Users\Richtern\Documents\MATLAB\Layer Prog\*.mat');
    load(char(fname))
    N=length(T_fq);
    dt=T_fq(2,1)-T_fq(1,1);
end

entry_val=input('What layer configuration echo path would you care to use?(0-->
    Full Echo, 1-->Validation, 2-->Echo Test, or 3--> Default)');

if entry_val==1

```

```

mat= [2.99    0.148    1        0.000275    2;...
      2.54    0.597    2.2    0            1;...
      2.99    0.148    1        0.000275    2];

clear ET

ET = [3 0 1 0 NaN NaN NaN NaN NaN NaN;...
      5 0 1 2 1 0 NaN NaN NaN NaN;...
      7 0 1 2 1 2 1 0 NaN NaN];

elseif entry_val==2

    mat= [9.70    0.148    1        0.000275    2;...          Layer 1
          1.00    0.4      1.5      0            1;...          Layer 2
          1.70    0.4      2.25    0            1;...          Layer 3
          9.70    0.148    1        0.000275    2];%          Layer 4

    clear ET

    load echotest2

elseif entry_val==0

    if GC=='N'

        clear ET

        load ETrain

    end

end

end

face=input('At what interface should a defect be placed? Interface 1 exists
           between layers 1 and 2. Type 0 for no defect. ');

if face~=0

    MAT=zeros(size(mat,1)+1,size(mat,2));

    MAT(1:face,:)=mat(1:face,:);

    MAT(face+1,:)= [0.05    0.034029    0.001225    180    2.3];%Air filled
                    delamination

    MAT(face+2:end,:)=mat(face+1:end,:);

    clear mat

    mat=MAT;

end

figure(1); plot(T_FQ(:,1),T_FQ(:,2))

```

```

%% Reference RT Calculations
Z1=v1_fq*rho1_fq;
Z0=v0*rho0;
TT_fq=4*Z0*Z1/(Z0+Z1)^2;
R_fq=(Z1-Z0)/(Z1+Z0);
RT_fq=TT_fq*R_fq;
RT=refl_tran(ET,mat);
RT_quo=(RT./RT_fq)';
%% FFT for Reference
T_fq(:,1)=T_FQ(:,1);
T_fq(:,2)=T_FQ(:,2).*10^(gain/20);

F_fq=(1/(N*dt))*fft(T_fq(:,2));
f(:,1)=s_space(1.0e-20,1/dt,N);
figure(2);plot(f,abs(F_fq))
f_cut=input('What is the desired frequency cut-off?');
f_max=find(f>f_cut-dt,1);
F_FQ=F_fq;
F_fq(f_max+1:N)=0;
figure(3);plot(f,abs(F_fq))
%% Path Calculations for Echo Paths

%Z_eqv_ref=ref_mat(1,1)+ref_mat(2,2)/ref_mat(1,2)*ref_mat(2,1);
%TOF_ref=2*(z0/v0+2.54/v1_fq);
S=size(ET,1);
[echopath,TOFpath,layer]=eqvpath(ET,mat);

if entry=='N' || entry_diff=='N'
    for i=1:length(f)
        for j=1:length(echopath)
            D_ref(i,:)=diff_cor(1,v0,f(i),ref_eqv,FL);
            D(i,j)=diff_cor(1,mat(1,2),f(i),echopath(j),FL);
        end
    end
end

```



```

    for i=1:size(D,2)
        D_quo(:,i)=D(:,i)./D_ref;
    end
elseif entry_diff=='Y'
    D_quo=1;
end

%% Attenuation Exponential for Echo Paths

if entry=='N' || entry_atten=='N'
    alpha(:,1)=ref_mat(1,4).*f.^ref_mat(1,5);
    alpha(:,2)=ref_mat(2,4).*f.^ref_mat(2,5);
    atten_exp_ref=exp(-2*alpha(:,1)*ref_mat(1,1)-2*alpha(:,2)*ref_mat(2,1));

    for j=1:size(layer,1)% A given reverb...
        old=1;
        for i=1:size(layer,2)%Product of Atten Exp for all layers of given reverb
            alpha=mat(i,4).*f.^mat(i,5);
            z_tot=mat(i,1)*layer(j,i);
            old=old.*exp(-alpha.*z_tot);
        end
        atten_exp(:,j)=old;
    end

    for i=1:size(atten_exp,2)
        atten_quo(:,i)=atten_exp(:,i)./atten_exp_ref;
    end

elseif entry_atten=='Y'
    atten_quo=1;
end

%% Product of Quotients
D_atten_prod=D_quo.*atten_quo;

%%

```

```

F(1:N,1:S)=0;
for i=1:length(RT_quo)
    if entry_atten=='Y' && entry_diff=='Y'
        F(:,i)=F_fq(:).*RT_quo(i);
    else
        F(:,i)=F_fq(:).*RT_quo(i).*D_atten_prod(:,i);
    end
end

for i=1:f_max-1
F(N-i+1,:)=conj(F(i+1,:));
end

figure(4);plot(f,abs(F))
%% IFFT of F
T_path=N*dt*ifft(F,N);
tt=linspace(T_FQ(1,1),T_FQ(end,1),N);
figure(5);plot(tt,real(T_path(:,:)))

T0_echo=T_FQ(1,1)+1e-2*round((TOFpath-TOF_ref)*1e2);
DT=abs(T_FQ(1,1)-T_FQ(end,1));
sum_T0_DT=T0_echo+DT;
maxT=max(sum_T0_DT);
minT=min(T0_echo);
t=(minT:0.01:maxT)';
for i=1:length(T0_echo)
    I=find(t>T0_echo(i)-0.5e-2,1);
    ind(i,:)=[I I+N-1];
end

for i=1:size(T_path,2)
    C_i=padarray(T_path(:,i),(length(t)-ind(i,2)),'post');
    C(:,i)=padarray(C_i,ind(i,1)-1,'pre');
end

T=sum(C,2);
figure(6);plot(t,T)

```

```

axis([min(t) max(t) -1 1])

xlabel('\musec')
ylabel('Response Amplitude')
if FL==7.5 && f0==5 && face==0
    title('Transducer A at 5 MHz without flaw')
    set(gcf, 'PaperPositionMode','auto',...
            'PaperUnits', 'inches',...
            'PaperSize', [6 5]);
    print('-dpdf','Tran_A_5u')
    saveas(gcf,'Tran_A_5u','fig')
elseif FL==7.5 && f0==5 && face~=0
    title('Transducer A at 5 MHz with flaw')
    set(gcf, 'PaperPositionMode','auto',...
            'PaperUnits', 'inches',...
            'PaperSize', [6 5]);
    print('-dpdf','Tran_A_5')
    saveas(gcf,'Tran_A_5','fig')
elseif FL==7.5 && f0==10 && face==0
    title('Transducer A at 10 MHz without flaw')
    set(gcf, 'PaperPositionMode','auto',...
            'PaperUnits', 'inches',...
            'PaperSize', [6 5]);
    print('-dpdf','Tran_A_10u')
    saveas(gcf,'Tran_A_10u','fig')
elseif FL==7.5 && f0==10 && face~=0
    title('Transducer A at 10 MHz with flaw')
    set(gcf, 'PaperPositionMode','auto',...
            'PaperUnits', 'inches',...
            'PaperSize', [6 5]);
    print('-dpdf','Tran_A_10')
    saveas(gcf,'Tran_A_10','fig')
elseif FL==8.5 && f0==5 && face==0%B
    title('Transducer B at 5 MHz without flaw')
    set(gcf, 'PaperPositionMode','auto',...

```

```

        'PaperUnits', 'inches',...
        'PaperSize', [6 5]);
print('-dpdf','Tran_B.5u')
saveas(gcf,'Tran_B.5u','fig')
elseif FL==8.5 && f0==5 && face~=0
    title('Transducer B at 5 MHz with flaw')
    set(gcf, 'PaperPositionMode','auto',...
        'PaperUnits', 'inches',...
        'PaperSize', [6 5]);
    print('-dpdf','Tran_B.5')
    saveas(gcf,'Tran_B.5','fig')
elseif FL==8.5 && f0==10 && face==0
    title('Transducer B at 10 MHz without flaw')
    set(gcf, 'PaperPositionMode','auto',...
        'PaperUnits', 'inches',...
        'PaperSize', [6 5]);
    print('-dpdf','Tran_B.10u')
    saveas(gcf,'Tran_B.10u','fig')
elseif FL==8.5 && f0==10 && face~=0
    title('Transducer B at 10 MHz with flaw')
    set(gcf, 'PaperPositionMode','auto',...
        'PaperUnits', 'inches',...
        'PaperSize', [6 5]);
    print('-dpdf','Tran_B.10')
    saveas(gcf,'Tran_B.10','fig')
elseif FL==9.5 && f0==5 && face==0%C
    title('Transducer C at 5 MHz without flaw')
    set(gcf, 'PaperPositionMode','auto',...
        'PaperUnits', 'inches',...
        'PaperSize', [6 5]);
    print('-dpdf','Tran_C.5u')
    saveas(gcf,'Tran_C.5u','fig')
elseif FL==9.5 && f0==5 && face~=0
    title('Transducer C at 5 MHz with flaw')
    set(gcf, 'PaperPositionMode','auto',...

```

```

        'PaperUnits', 'inches',...
        'PaperSize', [6 5]);
    print('-dpdf','Tran_C_5')
    saveas(gcf,'Tran_C_5','fig')
elseif FL==9.5 && f0==10 && face==0
    title('Transducer C at 10 MHz without flaw')
    set(gcf, 'PaperPositionMode','auto',...
        'PaperUnits', 'inches',...
        'PaperSize', [6 5]);
    print('-dpdf','Tran_C_10u')
    saveas(gcf,'Tran_C_10u','fig')
elseif FL==9.5 && f0==10 && face~=0
    title('Transducer C at 10 MHz with flaw')
    set(gcf, 'PaperPositionMode','auto',...
        'PaperUnits', 'inches',...
        'PaperSize', [6 5]);
    print('-dpdf','Tran_C_10')
    saveas(gcf,'Tran_C_10','fig')
else
    name=input('What is the desired title of the graph?','s');
    title(name)
    filename=input('What is the desired filename for the graph?','s');
    set(gcf, 'PaperPositionMode','auto',...
        'PaperUnits', 'inches',...
        'PaperSize', [6 5]);
    print('-dpdf',filename)
end

%sav=input('Save as...','s');
%save(sav,'t','T')

%Validation Outputs...
if entry_val=='Y'
    t_min=find(t>T_FQ(1,1)-dt,1);
    t_max=find(t>T_FQ(end,1)-dt,1);

```

```

figure;
subplot(2,1,1);plot(t(t_min:t_max),T(t_min:t_max),T_FQ(:,1),T_FQ(:,2),'ro')
legend('Multi-Layer Program','Transfer Matrix')
title('Time Responce')
xlabel('usec')
ylabel('Responce Amp')
FF=(1/(N*dt))*fft(T(t_min:t_max));
subplot(2,1,2); plot(f,abs(FF),f,abs(F_FQ),'ro')
legend('Multi-Layer Program','Transfer Matrix')
title('Frequency Responce')
xlabel('frequency(MHz) ')
ylabel('Responce Amp')
end

```

APPENDIX E. TRANSFER MATRIX PROGRAM

The following program computes the ultrasonic response through the use of the transfer matrix.

```
% Copyright (C)2003
% Iowa State University
% All Rights Reserved
%
% Written 05/03, Anxiang Li
% Modified 09/08, T. Gray
% Modified 01/10, N. Richter

% This program simulates the reflected and transmitted signals of a 5-layer
% structure immersed in water, with a infinite plane wave normally incident.

close all;
clear all;

%-----
%
% USER INPUT - define the incident pulse frequency and duration
%
f0=2.25; % Center frequency of incident pulse, MHz. *** USER INPUT
ncycles=2; % Number of cycles in incident pulse *** USER INPUT
dt = 0.01; % sampling rate in waveforms, microseconds *** USER INPUT
%
%-----
```

```

gain=input('What is the desired gain?');
Amp=1*10^(gain/20); % Peak amplitude of incident pulse
Npts=2^15; % # of sampling points.
t=linspace(0,(Npts-1)*dt,Npts)'; % time points, holds waveform.
df=1/(Npts*dt); % frequency increment in spectra, MHz
pulse_in = t*0.0;
pulsewidth = ncycles/f0; % duration of incident pulse
npulsewidth = pulsewidth/dt; % number of points in incident pulse
t0=linspace(0,pulsewidth,npulsewidth+1);
for m=1:npulsewidth+1
    pulse_in(m) = Amp*cos(2.0*pi*f0*t0(m))...
                *(1.0-((t0(m)-pulsewidth/2.0)/(pulsewidth/2.0))^2)
                ;
end;

figure(1); plot(t,pulse_in);
axis([0 10 -1 1])
axis([0,t(2*ceil(npulsewidth)),-max(abs(pulse_in)),max(abs(pulse_in))]);
xlabel('time (microsec)');title('Incident pulse');

f=(1:Npts)'\-1)*df;
fpulse_in = fft(pulse_in)*1/(dt*Npts);
% View the frequency spectrum of the incident pulse.
figure(2); plot(f(1:Npts/2+1),abs(fpulse_in(1:Npts/2+1)));
axis([0,2*f0,0,max(abs(fpulse_in))]);
xlabel('frequency (MHz)');title('Incident spectrum');
%-----
%
% USER INPUT - define the layer properties
entry=input('What layer configuration would you care to use?(0-->Full Armor, 1-->
    Validation, and 2-->Echo Test)');
entry_atten='N';
if entry==0.
    %Full Armor
    mat= [9.70    0.148    1        ;... Layer 1

```



```

1.68    0.336    1.78    ;... Layer 2
0.249    0.155    1.09    ;... Layer 3
0.378    0.302    1.59    ;... Layer 4
1.908    1.224    3.235    ;... Layer 5
0.378    0.302    1.59    ;... Layer 6
9.70     0.148    1        ];% Layer 7

elseif entry==1

    %Used as reference for Multi-layered Program to determine self
    %consistancy.

    mat= [2.99    0.148    1        ;... Layer 1
          2.54    0.597    2.2    ;... Layer 2
          2.99    0.148    1        ];% Layer 3

else

    %Used as to determine the need to model equivilent path collisions

    mat= [9.70     0.148    1        ;... Layer 1
          1.00     0.4      1.5      ;... Layer 2
          1.70     0.4      2.25     ;... Layer 3
          9.70     0.148    1        ];% Layer 4

end

%

density= mat(:,3);% densities in grams per cubic cm    *** USER INPUT
velocity= mat(:,2);% velocities in cm per microsecond  *** USER INPUT
thickness=mat(:,1);% thicknesses entered in cm         *** USER INPUT

%-----
% Acoustical parameters for the 5 layers. These parameters can be adjusted,
% but need to look at the number of frequency points, time range, etc. to
% make sure that the inverse Fourier transform gives correct results.

% The numbering of the layers
% incident wave --> |1|2|3|4|5|--> transmitted wave
% reflected wave <--

trsm.f(1)=0; % store the frequency spectrum of the transmitted wave .
reft.f(1)=0; % store the frequency spectrum of the reflected wave.

```

```

for m=2:Npts/2+1 % do the multiple frequency calculation.
    freq=(m-1)*df;
    V=velocity;
    Z=density.*V;
    Z_0=Z(1);
    k_0=2*pi*freq/V(1);
    kd=2*pi*freq./V.*thickness; % acoustical length (kXd) of each layer.
    % Transfer (ABCD) matrix components.

    A_layers=cos(kd);
    B_layers=1i.*Z.*sin(kd);
    C_layers=1i./Z.*sin(kd);
    D_layers=cos(kd);
    % total transfer matrix for the 5 layer structure.
    T=[1 0;0 1];
    for n=1:length(thickness)
        T=T*[A_layers(n) B_layers(n);C_layers(n) D_layers(n)];
    end;
    A=T(1,1);
    B=T(1,2);
    C=T(2,1);
    D=T(2,2);
    % change to scattering parameters using Z_0=characteristic impedance of
    % water.
    S11(m) = (A+B/Z_0-C*Z_0-D) / (A+B/Z_0+C*Z_0+D);
    S21(m) = 2 / (A+B/Z_0+C*Z_0+D);
    % calculate the frequency spectra of the transmitted/reflected wave
    % forms.
    trsm_f(m)=S21(m)*fpulse_in(m);
    reft_f(m)=S11(m)*fpulse_in(m);
end;

% fill the upper half of the spectrum with the complex conjugate of the
% lower half, to ensure a real wave form upon inverse FFT.
temp=fliplr(trsm_f(2:Npts/2));
trsm_f(Npts/2+2:Npts)=(temp') .';

```

```

temp=fliplr(reft_f(2:Npts/2));
reft_f(Npts/2+2:Npts)=(temp').';
trsm_t=ifft(trsm_f)*Npts*dt;
reft_t=ifft(reft_f)*Npts*dt;

% show the results.
figure(4); plot(t,real(trsm_t));axis([0,t(Npts),...
                                     -max(abs(real(trsm_t))),max(abs(real(trsm_t)))]);
grid on;
xlabel('time (microsec)'); title('transmitted wave');
figure(5); plot(t,real(reft_t));axis([0,t(Npts),...
                                     -max(abs(real(reft_t))),max(abs(real(reft_t)))]);
grid on;
xlabel('time (microsec)'); title('reflected wave');
axis([t(find(abs(reft_t)>1e-1,1)-100) max(t) -1 1])

%Output Arguments
mini=input('What is the t value for bound minimum?');
range=input('What is the t value for the range?');
t_min=find(t>mini,1);
t_max=find(t>mini+range,1);
TT=[t(t_min:t_max) real(reft_t(t_min:t_max))'];
save('valid_TM','TT')
entry2=input('Do you wish to save for validation?(Y/N)','s');
if entry2=='Y'
    T_FQ=[t(t_min:t_max) real(reft_t(t_min:t_max))'];
    figure(6); plot(T_FQ(:,1),T_FQ(:,2))

    save('validation','T_FQ')
end

```